Synthesis of multifunctional chlorhexidine-doped thin films for titanium-based implant materials

Adaias Oliveira Matos[a,b], Amanda Bandeira de Almeida[a], Thamara Beline[a], Caroline C. Tonon[c]; Renato Corrêa Viana Casarin[a], Lester Jack Windsor[b]; Simone Duarte[c]; Francisco Humberto Nociti Junior[a], Elidiane Cipriano Rangel[d], Richard L. Gregory[b]; Valentim Adelino Ricardo Barão[a,*]

[a] *Department of Prosthodontics and Periodontology, Piracicaba Dental School, University of Campinas (UNICAMP), Piracicaba, São Paulo, Brazil*

[b] *Department of Biomedical Sciences and Comprehensive Care, Indiana University School of Dentistry, Indianapolis, Indiana, USA.*

[c] *Department of Cariology, Operative Dentistry and Dental Public Health, Indiana University, Purdue University Indianapolis, School of Dentistry, Indianapolis, Indiana, USA.*

[d] *Laboratory of Technological Plasmas (LaPTec), São Paulo State University (UNESP), Science and Technology Institute of Sorocaba (ICTS), Sorocaba, São Paulo, Brazil*

***** Corresponding author.

E-mail address: vbarao@unicamp.br (V. Barão).

Declarations of interest: none.

This is the author's manuscript of the article published in final edited form as:

Matos, A. O., de Almeida, A. B., Beline, T., Tonon, C. C., Casarin, R. C. V., Windsor, L. J., Duarte, S., Nociti, F. H., Rangel, E. C., Gregory, R. L., & Barão, V. A. R. (2020). Synthesis of multifunctional chlorhexidine-doped thin films for titanium-based implant materials. Materials Science and Engineering: C, 117, 111289. https://doi.org/10.1016/j.msec.2020.111289

Abstract

Our goal was to create bio-functional chlorhexidine (CHX)-doped thin films on commercially pure titanium (cpTi) discs using the glow discharge plasma approach. Different plasma deposition times (50, 35 and 20 min) were used to create bio-functional surfaces based on silicon films with CHX that were compared to the control groups [no CHX and bulk cpTi surface (machined)]. Physico-chemical and biological characterizations included: 1. Morphology, roughness, elemental chemical composition, film thickness, contact angle and surface free energy; 2. CHX-release rate; 3. Antibacterial effect on *Streptococcus sanguinis* biofilms at 24, 48 and 72 h; 4. Cytotoxicity and metabolic activity using fibroblasts cell culture (NIH-F3T3 cells) at 1, 2, 3 and 4 days; 5. Protein expression by NIH-F3T3 cells at 1, 2, 3 and 4 days; and 6. Co-culture assay of fibroblasts cells and *S. sanguinis* to assess live and dead cells on the confocal laser scanning microscopy, mitochondrial activity (XTT), membrane leakage (LDH release), and metabolic activity (WST-1 assay) at 1, 2 and 3 days of co-incubation. Data analysis showed that silicon films, with or without CHX coated cpTi discs, increased surface wettability and free energy ($p<0.05$) without affecting surface roughness. CHX release was maintained over a 22-day period and resulted in a significant inhibition of biofilm growth ($p<0.05$) at 48 and 72 h of biofilm formation for 50 min and 20 min of plasma deposition time groups, respectively. In general, CHX treatment did not significantly affect NIH-F3T3 cell viability ($p>0.05$), whereas cell metabolism (MTT assay) was affected by CHX, with the 35 min of plasma deposition time group displaying the lowest values as compared to bulk cpTi ($p<0.05$). Moreover, data analysis showed that films, with or without CHX, significantly affected the expression profile of inflammatory cytokines, including IL-4, IL-6, IL-17, IFN-y and TNF-α by NIH-F3T3 cells ($p<0.05$). Co-culture demonstrated that CHX-doped film did not affect the metabolic activity, cytotoxicity and viability of fibroblasts cells ($p>0.05$). Altogether, the findings of the current study support the conclusion that silicon films added with CHX can be successfully created on titanium discs and have the potential to affect bacterial growth and inflammatory markers without affecting cell viability/proliferation rates.

Key words:

Chlorhexidine

Titanium

Biocompatible

Antibacterial

Biofilm

Graphical Abstract

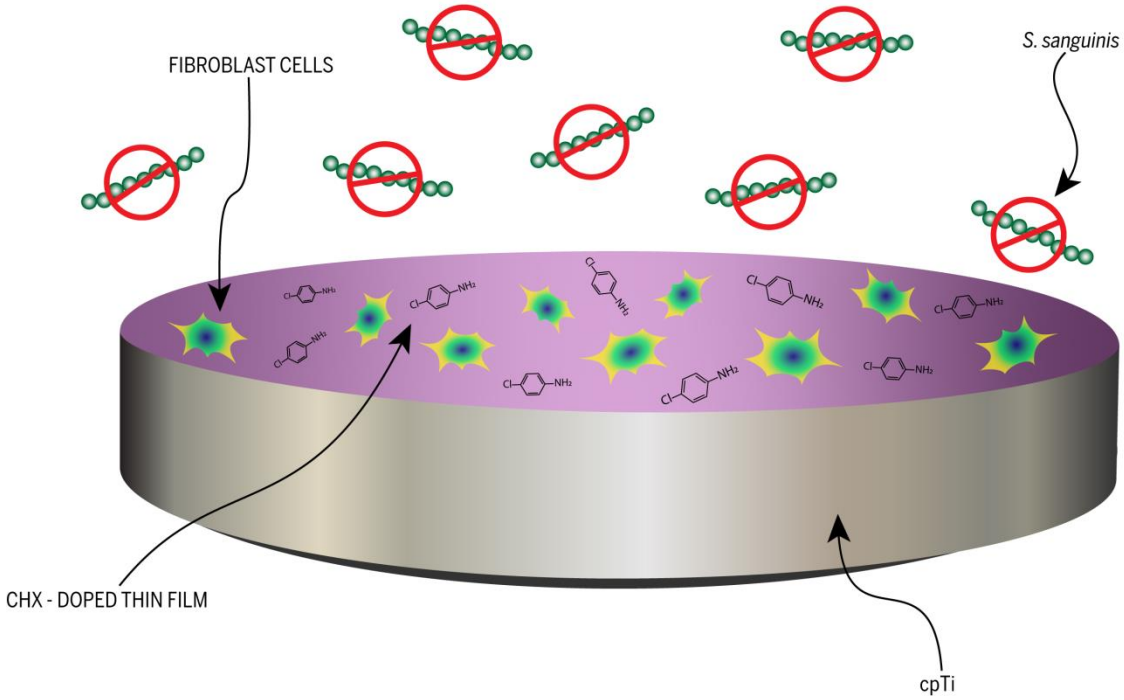

Highlights:

- CHX-doped thin films were successfully created.
- Created films were able to release CHX over 22 days.
- Films containing CHX inhibited biofilm formation without affecting host cells.

1. Introduction

A stable relationship between dental implant, abutment and peri-implant oral tissues is a requirement for the long-term success of implant therapy [1]. Bacterial colonization has been suggested as a critical factor leading to peri-implant tissue inflammation and bone loss, which eventually impact on implant survival [2, 3]. Over the years, a number of studies have tried to create functional surfaces to control biofilm formation around titanium implants [4-6]. CHX is one of the most effective antimicrobial agents. It inhibits proteolytic and glycosidic activities, and reduces the action of metalloproteinases of oral bacteria [7, 8], displaying a broad antibacterial effect against gram-positive and gram-negative microorganisms.

Several studies have sought to modify the surfaces of dental implants and prosthetic components using CHX to control bacterial colonization on the titanium surface. Such an agent-releasing approach is a promising strategy because the antimicrobial effect provided by the drug can go further to the specific site where it is localized [9]. Different approaches have been used to incorporate CHX into titanium surface including the technique of air-polishing with CHX powder [10], grated method with CHX [11], and the incipient impregnation method followed by solvent evaporation [12, 13]. However, discouraging findings have been reported which includes the absence of an antibacterial effect on mature biofilms.

Low-pressure glow discharge plasma (GDP) is a promising method to create biofunctional surfaces at low temperature [14, 15]. Plasma deposition of thin films using organosilicon precursors, such as hexamethyldisiloxane (HMDSO), results in high deposition rates in addition to allowing control of the structure and properties of surface films by varying deposition conditions [16]. Thus, surface modification using the GDP approach has the potential to modify material's properties allowing the introduction of various functional groups [17]. Organosilicon films can be deposited by exposing HMDSO compound to GDP. We hypothesized that the addition of CHX to the process may lead to the incorporation of this compound into the developing surface through homogeneous (plasma phase) and heterogeneous (surface plasma) reactions, and the incorporation of CHX onto metallic surfaces has the potential to create antimicrobial dental implant components to modulate biofilm formation, and therefore, affect peri-implantitis installation. In the current study, we used for the first time GDP as a new route to create a CHX-doped thin film on the surface of titanium-based materials and their physico-chemical, biological and antibacterial properties were defined.

2. Materials and methods

2.1. Experimental Design

Commercially pure titanium (cpTi) discs, 10 mm in diameter and 2 mm thickness, were randomly divided and submitted to GDP treatment. Three distinct experimental surfaces containing CHX were created by varying plasma deposition time (50, 35 and 20 min). Thin films without CHX and bulk cpTi discs (machined surface) were used as positive and negative controls, respectively. Physico-chemical characterization included surface morphology and roughness, elemental chemical composition, film thickness, CHX-release, contact angle and surface free energy. Antimicrobial properties of the experimental surfaces were assessed at 24, 48 and 72 h in early and later colonization of *Streptococcus sanguinis*, and assays included the number of viable microorganisms and live/dead cells. Furthermore, fibroblasts cell culture (NIH-F3T3) was used to determine the impact of CHX-treated surfaces on cell viability, morphology and expression of inflammatory markers at 1, 2, 3 and 4 days. Co-cultures of human periodontal ligaments fibroblast cells and *S. sanguinis* were analyzed through metabolic activity (WST-1 assay), mitochondrial activity (XTT), membrane leakage (LDH release) and confocal laser scanning microscopy (CLSM) (LIVE/DEAD) assays. Summary of experimental design is illustrated in Figure 1.

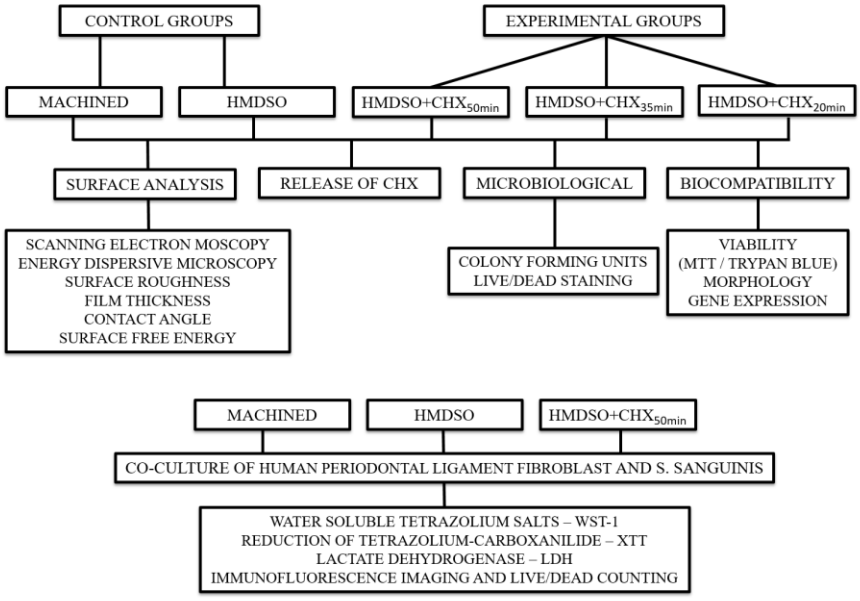

Fig. 1. Flowchart of experimental procedures. Bulk cpTi (machined) and GDP-created films based on silicon (HMDSO) without CHX were used as negative and positive controls, respectively.

2.2. Disc preparation

CpTi discs (Grade II; MacMaster Carr) [composition in wt% was Ti (99.7), C (0.006), Fe (0.12), O_2 (0.16), N_2 (0.004), and H_2 (0.0019)] were polished with a sequential SiC abrasive papers (#320, #400, #600 and #800) (Carbimet 2; Buehler), ultrasonically cleaned with deionized water and detergent (Det limp 32, Chemco), degreased with acetone and air-dried. Non-GDP-treated surfaces (machined) were considered as the negative control group.

2.3. Glow discharge plasma (GDP) treatment

A custom-made steel reactor was used for GDP treatments (Technological Plasma Laboratory; São Paulo State University, Brazil). In all cases, film deposition was performed in an atmosphere containing HMDSO (85%) and argon (15%) at a working pressure of 4.0×10^{-2} Torr (2.0×10^{-2} of base pressure). In three of the deposition procedures, 0.8 g of chlorhexidine diacetate salt hydrate powdered (CHX) (Sigma-Aldrich) was placed onto the driven lowermost electrode. Plasma deposition was performed using radio frequency signal (13.56 MHz, 150 W) applied to the lower electrode while the topmost sample holder was earthed. Three different silicon-based films were produced in the presence of CHX by varying the plasma deposition time to the following: 15, 30 and 45 min. Such plasma deposition time variation was an attempt to provide the incorporation of different concentrations of CHX in the silicon film. After each deposition cycle, the flux of the precursor compound (HMDSO) was interrupted in a way that plasma was sustained only by Ar flux. This final process, which provoked Ar ion bombardment only, lasted 5 min in all cases and was not applied for the preparation of the control sample (free of CHX). No CHX was added to the deposition process in order to prepare the positive control group (HMDSO). In this case, time of deposition was 15 min. Thus, the name of each thin film group was based on the total exposure time to the plasma process (deposition + Ar bombardment), as shown in table 1.

Table 1
Name of groups based on silicon-based films time.

Name of groups	Silicon-based films time		
	HMDSO + Ar	CHX	Ar bombardment
HMDSO	15 min	No	No
HMDSO+CHX_{20min}	15 min	Yes	5 min
HMDSO+CHX_{35min}	30 min	Yes	5 min
HMDSO+CHX_{50min}	45 min	Yes	5 min

2.4. Surface characterization

Surface morphology and topography were determined by scanning electron microscopy (SEM) (JEOL JSM-6010LA; JEOL), whereas energy dispersive spectroscopy (EDS) was used to define surface chemical composition (n=10) [18]. Surfaces were sputtered with Au-Pd alloy and micrographs were obtained using secondary electrons detector and beam energy of 3.0 keV. A profilometer (Veeco, Dektak 150) was used to assess surface roughness (n=10) and film thickness (n=4) using a 500-μm scan for 15 s and a load of 3 mg. Each specimen was scanned at least 5 times before and after film deposition. Four different parameters of surface roughness were obtained: average roughness (Ra), root mean-square-average (Rq), average maximum height of the profile (Rz), and maximum height (Rt). In order to measure film thickness, plasma was deposited onto a glass slide partially coated with a Kapton adhesive tape to create a step. Moreover, wettability and surface energy were determined by an automatic goniometer (Ramé-Hart 100-00; Ramé-Hart Instrument Co) (n=10). Two liquids were used (water as a polar component and diiodomethane as a dispersive component) and their contact angle with the surface was measured. The relation between contact angle and surface energy was evaluated by the Owens-Wendt method [19].

2.5. Chlorhexidine release

CHX release rate was determined by UV absorbance. Each sample was immersed in ultrapure deionized water (⩾18.2 MΩ cm) (Advance A10 Milli-Q system, Millipore) (2 mL), and 200-μL aliquots were collected at 24 h intervals for 22 days. An equal amount of fresh deionized water was added back to the elution solution following each aliquot retrieval time

point and a standard curve was obtained from a series of concentrations of CHX. UV absorbance was measured at 300 nm wavelength using a UV spectrophotometer (Spectra Max 190). CHX release rate for each group was determined using linear regression equations obtained from the calibration curve ($r^2 > 0.99$) [20].

2.6. Antibacterial analysis

For all biological analysis, discs were sterilized by gamma radiation (14.5 ± 0.05 kGy) [21]. In this study, *S. sanguinis* reference strain (IAL 1832) was used. Detailed preparation of the inoculum is described elsewhere [22]. Pooled unstimulated human saliva, provided by two healthy volunteers (register number CAAE: 57499416.9.0000.5418), was centrifuged at 10,000 *g* for 10 min at 4 °C and the supernatant was sterilized under filtration [23]. For salivary pellicle formation, cpTi discs were coated with 1 mL of saliva and incubated for 2 h at 37 °C. Afterwards, saliva was aspirated and 100 μL of an *S. sanguinis* cell suspension (10^7 cells/mL) and 900 μL of BHI broth supplemented with 1% glucose were added. Plates were incubated in 10% CO_2 at 37 °C for 24, 48 and 72 h. The medium was refreshed every 24 h. Assays were performed at least 3 times in triplicate (n=9). After biofilm formation, discs were washed with 0.9% NaCl to remove non-adherent cells, and adherent cells were removed under sonication (7 W for 30 s) in 0.9% NaCl. Sonicated suspensions (20 μL) were serial diluted and plated in triplicate onto Trypticase Soy Agar (TSA) (Difco Laboratories) and incubated at 37 °C in 10% CO_2 for 48 h to determine the number of colony forming units (CFUs). Data were expressed as Log_{10} CFU/mL. Additional biofilm-containing discs (n=2) were analyzed under a confocal laser scanning microscope (Leica Microsystems CMS, Mannheim, Baden-Württemberg, Germany) at 40× magnification. Biofilm was stained with LIVE/DEAD bacterial viability kit (Life technologies) where live bacteria appear in green (Syto®9) and dead bacteria appear in red (Propidium Iodide) [24].

2.7. Cell culture and biological analyses

NIH-F3T3 cells were cultivated in Dulbecco's Modified Eagle's Medium (DMEM) supplemented with 10% fetal bovine serum (FBS) (Gibco, Life Technologies) and antibiotics (100 mg/mL of streptomycin and 100 U/mL of penicillin). A total of 3×10^4 cells/well was seeded in 24-well plates containing or not cpTi discs with or without CHX. After 24 h, medium was replaced with DMEM supplemented with 2% FBS and antibiotics (day 0), and was replaced at 48 h. Experiments were performed twice in triplicate. Cell metabolic activity was determined by the MTT assay [25] at 1, 2, 3 and 4 days according to the manufacturer's

instructions. Briefly, culture medium was replaced by 900 µL of DMEM supplemented with 100 µL of MTT (5 mg/mL) (Life Technologies) at 37 °C, and 5% CO_2 and incubated for 4 h, under dark condition. Supernatants were removed and replaced with 2 mL of 100% alcohol (Sigma-Aldrich) to dissolve the formazan crystals. Optical density of the solution was read at 570 nm (VersaMax; Molecular Devices). Cell viability was assessed by the trypan blue dye exclusion method. At each experimental period (1, 2, 3 and 4 days), 10 mL of 0.4% trypan blue was prepared, cells were washed with phosphate buffer solution (PBS) at 37 ºC, trypsinized with 3-5 mL of culture medium and neutralized with 3-5 mL of PBS supplemented culture medium. Cells were transferred to a 15 mL tube and centrifuged for 5 min at 2,500 rpm, the supernatant was aspirated, and the pellet resuspended in 1 mL of PBS. A total of 20 µL of the cell suspension was transferred to a microcentrifuge tube and 20 µL of the trypan blue was added. Cells were incubated for 5 min at room temperature and stained and non-stained cells were counted as non-viable and viable cells, respectively. In order to determine the impact of CHX containing surfaces on NIH-F3T3 cell morphology, 3×10^4 cells/well were seeded in 24 well culture plates for 1, 2, 3 and 4 days. After the experimental periods, cells were fixed in Karnovsky's solution for 12 h at 4 °C and post-fixed in 1% osmium tetraoxide for 1 h at room temperature protected from light [21]. Cells were dehydrated in ethanol series (35, 50, 70, 90 and 100%) at room temperature for 10 min each. After the final dehydration, samples were critical-point dried (Denton Vacuum, mod. DCP-1) and gold sputter treated (Bal-Tec, mod. SCD 050) [21] for SEM analysis.

2.8. Secretome assay

In order to determine the impact of CHX containing surfaces on the expression of inflammatory markers, 3×10^4 cells/well were seeded in 24 well culture plates containing or not cpTi discs with or without CHX for 1, 2, 3 and 4 days. After the experimental periods, secreted levels of the interleukin (IL)-4, IL-6, IL-17, tumor necrosis factor (TNF)-α, and interferon (IFN)-γ were determined using the multiplexing technology following a previous protocol [26].

2.9. Co-culture and analyses of fibroblast cells and S. sanguinis

To investigate further the clinical significance of the CHX-doped film developed herein, a co-culture model of fibroblast cells and *S. sanguinis* was investigated. A total of 100 µL of an overnight culture of *S. sanguinis* (ATCC 10556) was mixed with 5 mL of brain heart infusion (BHI) broth (Difco Laboratories, Becton, Dickinson and Company)

supplemented with 1% of glucose and incubated overnight. Then, 1 mL of the growth medium was transferred to 9 mL of BHI broth supplemented with 1% of glucose for 3 h in 5% CO_2 (v/v) at 37 °C without agitation. Afterwards, *S. sanguinis* cells were harvested by centrifugation (6,000 *g* for 5 min at 4 °C), washed twice with 0.9% NaCl and were resuspended in DMEM. A final suspension of 10^7 cells/mL was adjusted by a spectrophotometer (Spectronic 20; Bausch & Lomb) at 600 nm (OD = 1 ±0.02) [22]. Human periodontal ligament fibroblast cells (HPLF) were cultured in DMEM supplemented with 10% fetal bovine serum (FBS) (Gibco, Life Technologies), penicillin (100 U/mL), and streptomycin (100 mg/mL; Gibco, Life Technologies). Cells were incubated for 24 h at 37 °C in a humidified atmosphere of 95% air and 5% CO_2. After 24 h, medium was replaced with Alpha MEM supplemented with 2% FBS (day 0), and was replaced every other day until the end of experimental period. Once the microorganisms were added to the cell culture, antibiotics were not added to the medium, to avoid interference in the biofilm development. The direct interaction between bacteria and fibroblast cells was investigated in 24-well plates. The multiplicity of infection (MOI) of 1:100 bacteria/cell was calculated based on the total number of cells per well at confluence [27]. Then both human periodontal ligament fibroblast cells and *S. sanguinis* suspensions were propagated onto cpTi discs and incubated for 24, 48 and 72 h at 37 °C and 5% CO_2. After that, the growth medium was replaced with fresh DMEM without antibiotics every 24 h until the end of the experimental period. After each time of incubation, the co-culture medium of each sample was collected, transferred to a 96-well microtiter plate (100 µL of culture medium per well, totalizing 6 measurements for each sample) and cooled to room temperature, then the WST-1, XTT and LDH tests were performed. All analyses were performed in triplicate and the mean values of the three different readings were used for statistical comparisons. Non-treated fibroblast cells (cells seeded onto 24-well polystyrene plates without titanium discs) were used as a control of the experiment.

The metabolic activity from the co-cultures was tested using the cell proliferation WST-1-Kit (Roche Diagnostics GmbH). The conversion of tetrazolium salt via mitochondrial succinate-dehydrogenase-vital cells to colored formazan was measured spectrophotometrically. The co-cultures were gently washed twice with PBS; after each time of incubation (24, 48 and 72 h), 500 µL WST-reagent was added per well, and incubated for 4 h in the dark at 37 ºC. The absorbance at 450 nm was measured in a 96-well microtiter plate by a spectrophotometer. The percentage of metabolic activity was calculated using the following formula: metabolic activity (%) = (OD in treatment group/OD in control

group) × 100 [28]. This assay measured the mitochondrial activities of the co-culture based on the reduction of tetrazolium-carboxanilide (XTT; Sigma-Aldrich).

The XTT salt solution was prepared and activated with menadione. The co-culture was gently washed twice with PBS; 200 µL of the reaction mixture was added per well and incubated for 2 h in dark at 37 ºC. The absorbance at 490 nm was measured in a 96-well microtiter plate by a spectrophotometer after 24, 48 and 72 h [29]. The percentage of metabolic activity was calculated.

An LDH assay measured membrane leakage of LDH from the co-culture by an LDH Kit (Promega). Then, the kit reagent was added to each well (100 µL per well) and incubated for 45 min. After the addition of stop solution (50 µL per well), the signal was measured by a spectrophotometer at 590 nm. The percentage of viability was calculated using the following formula: viability (%) = (OD in treatment group/OD in control group) × 100 [28].

Co-cultures grown on cpTi discs were analyzed by qualitative visualization of live and dead bacterial stain. Discs were washed with PBS and placed in 24-well culture plates. Afterwards, a LIVE/DEAD® Bac Light Bacterial Viability kit (Sigma-Aldrich, USA) was used. The stained co-culture was visualized by a CLSM (Leica TCS SP5 Confocal Laser Scanning Microscope). The green nucleic acid SYTO 9 stain stains all cell populations, including those bacteria with intact and damaged membranes, whereas the red nucleic acid stain, propidium iodide, penetrates through damaged cell membranes. Thus, live bacteria were stained green and dead bacteria were stained red in the CLSM images. For quantification of live and dead bacteria, an intensity of interest was defined in a certain target by Imaris software (Bitplane, Inc., Saint Paul, MN, USA)) to control the heterogenous distribution of fluorescence labelling. Volume of intensity represents the number of voxels in the XYZ positions. The intensity of the sum of green or red bacteria were transformed and expressed as log values.

2.10. Statistical analysis

For the statistical analysis, the normality of errors (Shapiro-Wilk test) and homogeneity of variances (Levene test) were evaluated for each dependent variable. One-way ANOVA was used to investigate the effect of surface type on the roughness (Ra, Rq, Rt, Rz), film thickness, contact angle, surface free energy and antibacterial potential. Two-way ANOVA was used to evaluate the effect of surface type and time on the MTT, cell viability, release of interleukins assays, and co-culture assays (WST, XTT and LDH). Tukey HSD

post-hoc test was used to determine the level of significance between groups at a 95% confidence interval (SPSS v. 20.0; SPSS Inc).

3. Results and Discussion

3.1. Surface morphology and chemical composition

Secondary electron micrographs have shown that the plasma deposited film is a matrix evenly distributed on the surface containing surface particulate matter when CHX is added to the process (Fig. 2). The lower magnification (×300) of micrographs demonstrated film deposition onto the entire surface of titanium and the absence of cracks or discontinuities. The HMDSO group exhibited a smooth and uniform surface while the CHX-doped film exhibited the presence of some small particles sparsely distributed onto the surface are noted as a result of the CHX deposits. Longitudinal grooves were observed in the machined group as a consequence of the polishing process. In the ×2000 magnification, the presence of particulate structures was clearly observed over the entire surface in all groups prepared with the presence of CHX, appearing in higher amounts for the HMDSO+CHX_{20min} group. The HMDSO+CHX_{50min} and HMDSO+CHX_{35min} groups exhibited smaller particulate structures, which were grouped in specific areas.

The results of the elemental composition of the samples, derived from the EDS analysis, are presented in Fig. 3. Oxygen (O), carbon (C) and titanium (Ti) were detected onto machined surface. In this study, the plasma polymerized thin film was deposited onto titanium using HMDSO, and argon with and without the presence of CHX. The HMDSO group contained oxygen (O), carbon (C), and silicon (Si) peaks, consistently with the deposition atmosphere and similar to previous studies [21, 30]. All groups with films based on silicon with CHX exhibited peaks of oxygen (O), carbon (C), silicon (Si), chlorine (Cl) and sodium (Na). Silicon is one of the elements characteristic of organosilicon plasma deposited films [$(CH3)_2SiOSi(CH3)_2)_n$] due to fragmentation of hexamethyldisiloxane into methylsilyl groups and other reactive functionals which can be considered precursors for film formation [31]. Chemically, CHX is a synthetic cationic bis-biguanide composed of two chloroguanide chains linked through a central hexamethylene chain, exhibiting $C_{22}H_{30}Cl_2N_{10}$ as chemical formula [32]. In this study, the time of plasma deposition plays an important role in the CHX concentration (represented by the Cl element).

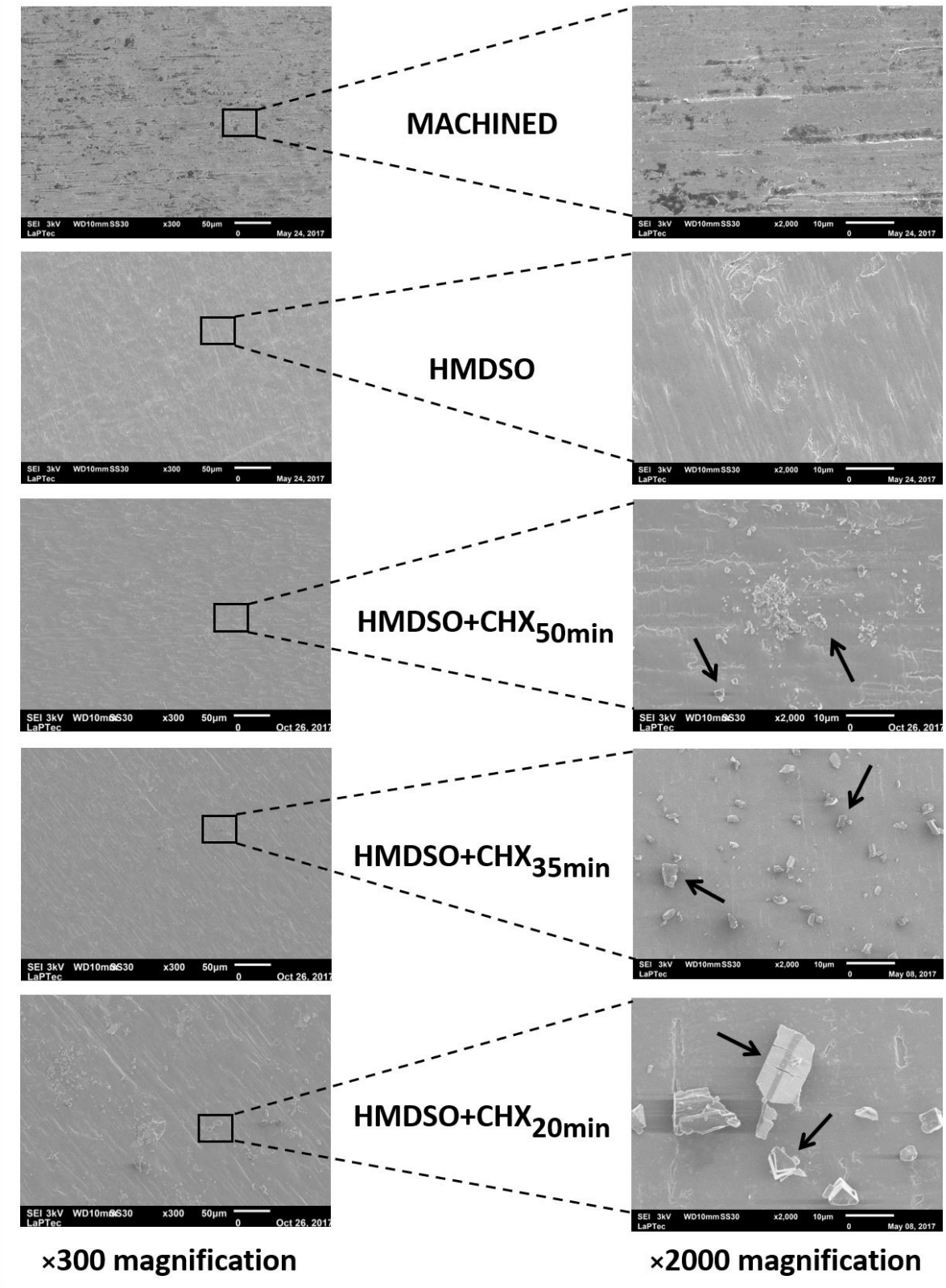

Fig. 2. Scanning electron micrographs of the surfaces of control and experimental groups at ×300 and ×2000 magnifications. Arrows indicate the presence of particulate structures representing the CHX deposits.

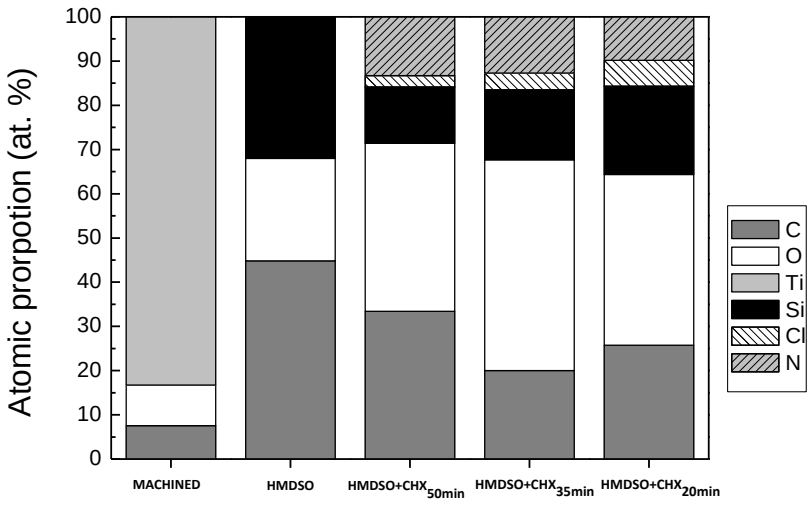

Fig. 3. Atomic proportion of the elements detected on the surface from EDS analysis for machined and experimental groups (n=10).

In the last five minutes of the process, when the flow of the precursor compound (HMDSO) was interrupted, the plasma consisted predominantly of argon. In this condition, the deposition process was interrupted, with low energy ion bombardment of the directed electrode prevailing, a process that intensifies the inclusion of CHX fragments into the plasma phase. It is interesting to note that even with this procedure, in which it was expected to incorporate the same proportion of Cl in all surfaces, regardless of the deposition time, there was a tendency for the proportion of this element to decrease with the increase in the deposition time. This behavior can be a consequence of the removal of CHX fragments from the film, in the final 5 min of the process. Although it is in contact with the grounded electrode, the titanium was coated with an electrically insulating film. Even so, electrons, which are species with high mobility, can continually collide with the surface of the insulating material present there, making it negatively charged, which attracts argon ions. The low energy ion bombardment thus induced can eject CHX fragments incorporated in the film deposition process. This mechanism, proposed by Yasuda [33], and schematized by Rangel et al. [34], would be favored in this research by the increase in the free mean electron path caused by the interruption in the flow of HMDSO. It would also explain the reduction in the Cl ratio of the surface if the sputtering time were increased. As the time of the sputtering process was kept constant in all experiments (last 5 min), the reduction in the atomic proportion of Cl was more consistent with the fact that the film was also deposited on CHX, making its emission to the plasma phase increasingly difficult as the deposition time grew.

3.2. Surface roughness and film thickness

The surface profiling has an important role in microbial adhesion and biofilm development [35, 36], and also affects the adhesion and proliferation of fibroblast cells [37]. Surface average roughness (Ra) for control and experimental groups was maintained below a 0.2 μm threshold. According to the roughness results presented in Fig. 4a, all groups displayed similar Ra, Rq, Rz and Rt values ($p>0.05$). Such roughness homogeneity among groups is an important aspect to reduce bias in the microbiological and biocompatibility assays and to investigate the real effect of each CHX concentration.

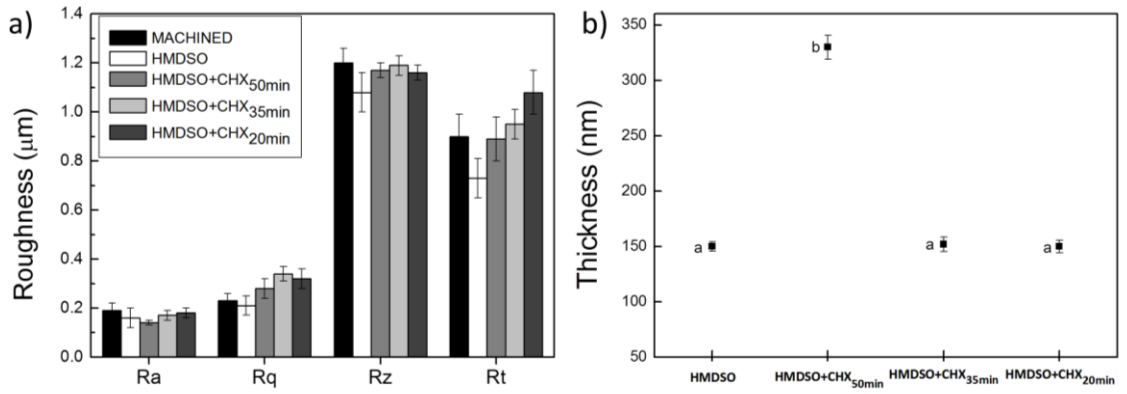

Fig. 4. (a) Roughness values (Ra, Rq, Rz, and Rt) for controls and experimental groups (n=10). Similar surface roughness was noted among groups ($p>0.05$). **(b)** Thickness of deposited thin films in the silicon-based films with and without CHX (n=4). Different letters indicate significant differences among groups ($p<0.05$). The error bars indicate standard deviation.

The thicknesses of the deposited films are shown in Fig. 4b. The HMDSO+CHX_{50min} group presented a statistically significant thicker film value (330 nm) when compared to the other groups (about 150 nm) ($p<0.001$). It has being reported that the plasma deposition time affects the film thickness [31]. Herein, the 50-min plasma deposition process generated a 330-nm film thickness while the 20- and 35-min coating process, reduced the film thickness in approximately 55% (thickness of 150 nm). The very thin thicknesses of coatings obtained by this plasma technique is an advantageous feature to avoid misfit in abutment and dental implant interface [38].

3.3. Wettability and surface free energy

The surface wettability of biomaterials is an important factor in the interaction of biomaterial/host interface [39]. Surface chemical composition, surface energy, surface water contact angle may in turn influence the material's biocompatibility [40]. In this study, a reduced water contact angle was noted for all coated groups, where all thin films based on silicon with or without CHX demonstrated statistically significant lower mean contact angles values (i.e. greater wettability) than the machined group ($p<0.05$). Consequently, all thin film groups presented higher mean surface free energy ($p<0.05$) (Fig. 5). Contact angle and surface free energy was not affected by the incorporation of CHX. Thus, the increase in wettability is attributed to the presence of silicon in the film.

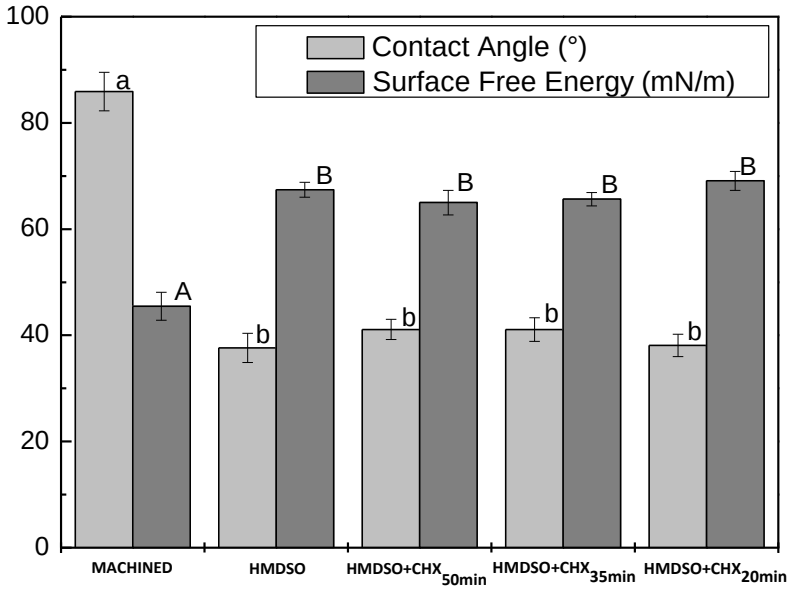

Fig. 5. Contact angle and surface free energy for controls and experimental groups (n=10). Different letters indicate statistical difference among groups for each dependent variable ($p<0.05$). Lower case letters were used for comparing contact angle values among groups. Capital letters were used for comparing surface free energy among groups. The error bars indicate standard deviation.

Surfaces with contact angles of water below 90° exhibit hydrophilic behavior, so that polar liquid is spread over the surface indicating greater surface wettability [41]. The hydrophilic nature and the high surface energy dictate the interaction between body fluids and biomaterials. For instance, in biological terms, cells dispersed in the body fluid should neighbor the implant surface to improve the attachment and proliferation of fibroblast-like

cells [42]. During film deposition, the argon gas generates hydroxyl polar groups onto the surface, which plays a role in increasing the surface free energy [43].

3.4. Evaluation of chlorhexidine release rate

CHX release rate was investigated over a 22-day period (Fig. 6). Data analysis indicated a slow release rate for CHX over 22 days until the CHX release peaked at day 8 in the HMDSO+CHX_{50min} and HMDSO+CHX_{35min} groups. On the other hand, the HMDSO+CHX_{20min} group featured a rapidly release with a peak at day 6 followed by a gradual reduction in CHX release over the remaining days. We speculate that a thicker film in the HMDSO+CHX_{50min} group and also having the lowest concentration of the chlorine element may have been the driven force toward its slower CHX release rate. Data of the current study suggest that the use of CHX-doped film onto metallic materials has the advantage to allow for a continuous and slow release of CHX, which is not possible using conventional approaches or rinses [13]. The kinetic release assays have revealed the proper behavior of this coating in terms of its gradual release of CHX, which was also shown to impact on *in vitro* biofilm formation. Although, promising findings are reported by the present study, further *in vivo* studies should be designed to determine whether or not CHX-doped films are able to affect biofilm development around dental implants, and more importantly, prevent peri-implantitis to occur.

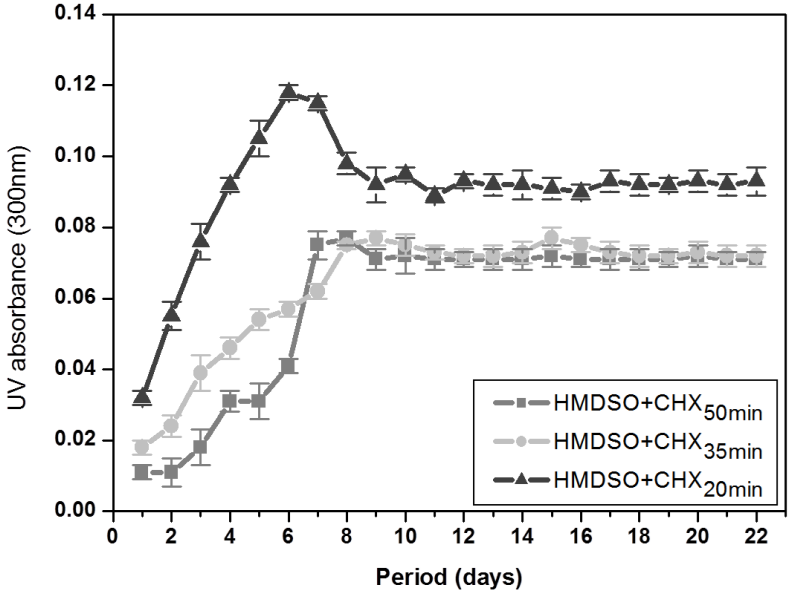

Fig. 6. Dynamics of CHX release from cpTi discs doped with different concentrations of chlorhexidine (n=2). Error bars indicate standard deviation.

3.5. Antibacterial behavior

The ability of CHX-doped films to affect early and late colonization of *S. sanguinis* (Log_{10} CFU/mL) was assessed at 24, 48 and 72 h and is illustrated in Fig. 7. Data analysis show that CHX containing surfaces present a trend to reduce biofilm formation. Significantly reduction was noted at 48 h of biofilm formation for HMDSO+CHX_{50min} vs. machined control ($p=0.04$). For more mature biofilm, HMDSO+CHX_{20min} exhibited lower Log_{10} CFU/mL counts than controls ($p<0.05$).

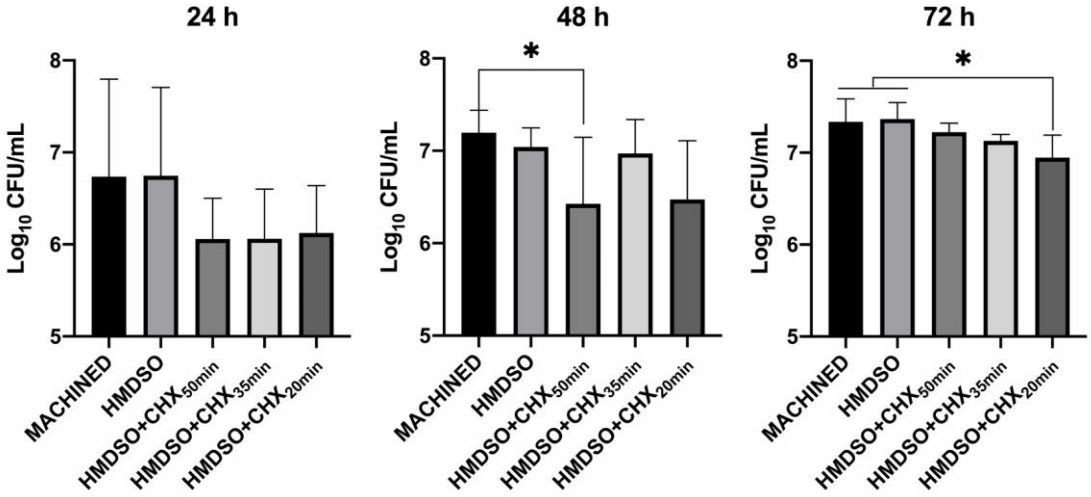

Fig. 7. Colony forming units (Log_{10} CFU/mL) of *S. sanguinis* for controls and experimental groups at 24, 48 and 72 h of biofilm development (n=9). The statistical difference between groups is showed with the connected line (*$p<0.05$). The error bars indicate standard deviation.

The effectiveness of CHX as an adjunct for periodontal therapy has been proven for many years. It modifies the periodontal microflora and inhibits glycosidic and proteolytic activities from potent periodontal pathogens [44, 45]. The results presented here demonstrate a suitable biofilm inhibition for CHX-doped films. The antimicrobial activity of CHX relies on the increased cellular membrane permeability and subsequent coagulation of intracellular cytoplasmic macromolecules [46]. In addition, the binding process between the CHX molecules and the lipoteichoic acid of gram-positive bacteria promotes the leakage of intracellular compounds and consequent bacterial death [47]. Although the HMDSO+CHX_{50min} group displayed the lowest and slowest drug releasing rate during the experimental period, it resulted in the highest level of biofilm inhibition during 48 h. Hugo and Longworth [48] found that low CHX concentrations led to a long period of

dehydrogenase activity (greater than 200 h), whereas as found in the current study higher concentrations of CHX are more rapidly bactericidal [48]. stages of biofilm formation (72 h) the HMDSO+CHX_{20min} group featured the greatest biofilm inhibition. We speculate that the antibacterial ability of CHX-doped films to inhibit biofilm formation has a direct relation with CHX concentration and the CHX particle size deposited onto the cpTi surface. For instance, SEM micrographs show that the HMDSO+CHX_{50min} exhibited smaller CHX particles while HMDSO+CHX_{20min} presented the greatest one. Lower particle size may induce a faster biofilm inhibition as shown here.

In the present work, additional experiments were carried out in order to define the antibacterial impact of CHX-doped films based on silicon created on cpTi. CLSM analysis demonstrated that CHX treatments possibly increased the number of dead cells (stained in red) as compared to the groups with no CHX (Fig. 8). These results confirm that CHX-doped films based on silicon created on cpTi discs have the potential to affect *S. sanguinis* viability, and consequently biofilm formation *in vitro*. In addition, these findings indicate that the CHX-doped film based on silicon approach has the advantage to affect biofilm formation at the early stages, which has been reported to be an advantage over the treatment of a well-structured mature biofilm [4]. It is important to point out that the reduced counts of *S. sanguinis* observed here was a valuable finding as our previous study [49] has shown that by reducing bacterial and fungal adhesion onto titanium surface, we were able to reduce the microbial dysbiosis changes and consequently the pathogenic potential of biofilms. Although the developed CHX-doped thin film is promising to reduce biofilm formation, future *in vitro* studies using more complex multi-species and *in situ* biofilm models are warranted. Additionally, even if there is biofilm reduction, it was lower than 1 $\log_{10}$ of CFU counts, so next studies should drive new protocols of CHX deposition to optimize its antimicrobial action without increasing toxicity or affecting its biocompatibility potential.

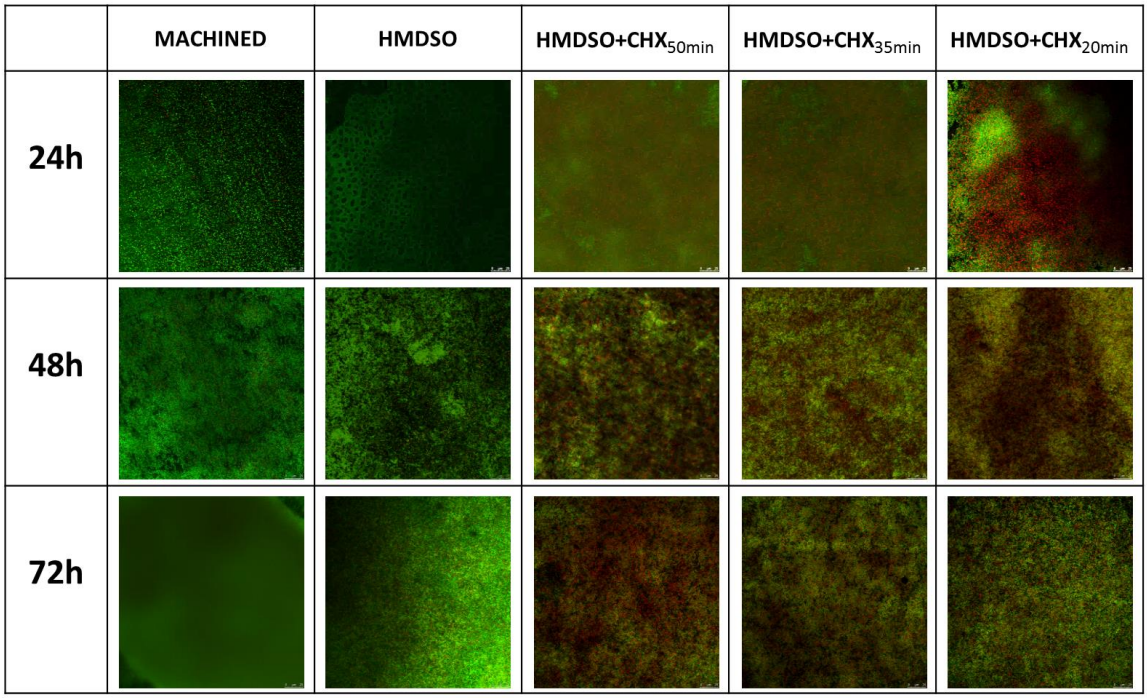

Fig. 8. Representative CLSM images of live/dead staining of *S. sanguinis* for control and experimental groups at 24, 48 and 72 h of biofilm development. Live cells are stained in green, whereas dead cells are stained in red.

3.6. Cell metabolic activity and viability/proliferation assays

In the current study, cell culture assays were performed in order to determine the impact of CHX-doped films created on cpTi discs on cell behavior. First, we assessed the effect of different silicon-based films, with or without CHX, on cellular metabolism by the MTT assay. In general, data analysis showed that GDP-created films alone significantly affected cell metabolism as compared to bulk cpTi at days 3 and 4. Interestingly, CHX treatment potentiated such effect at day 3. At the latter stages (day 4), CHX treatment did not alter the ability of cells to metabolize MTT compared to the film alone ($p>0.05$). Next, we examined the effect of CHX treatment on cell viability, and found a concentration dependent trend towards reduced viable cell numbers at day 3 ($p>0.05$) (Fig. 9b). Therefore, regardless of the plasma deposition time, CHX treatment did not significantly affect cell viability. Although, it has been suggested that treatment of peri-implant diseases with CHX could strive toxic effects on gingival fibroblasts and endothelial cells, mitigating the initial healing stage [50], the results of the present study indicate that a significant antibacterial effect of low concentration CHX-doped films based on silicon is possible without affecting the host cells. In addition, as forces underlying cell-matrix adhesive interactions may also be relevant to cell

responses, multiple measurement systems have been developed to quantify the spatial and temporal dynamics of cell adhesive forces, including washing the cells with physiologic buffers and counting the remaining cells afterward, as reviewed by Zhou & Andrés [51]. In the current study, as the proportion of viable cells was determined by counting the cells after washing control and experimental discs with PBS, one may assume that it also illustrates the impact of the substrate on cell adhesion strength. With that in mind, data analysis indicates that neither the control nor CHX-doped films significantly affected cell adhesion. However, our findings on cell adhesion should be cautiously interpreted, as such an approach presents limitations that include, for example, low sensitivity, and therefore, further studies should be designed using more contemporaneous assays including three-dimensional adhesion strength quantification, to further determine potential interferences of CHX-doped films on cell adhesion.

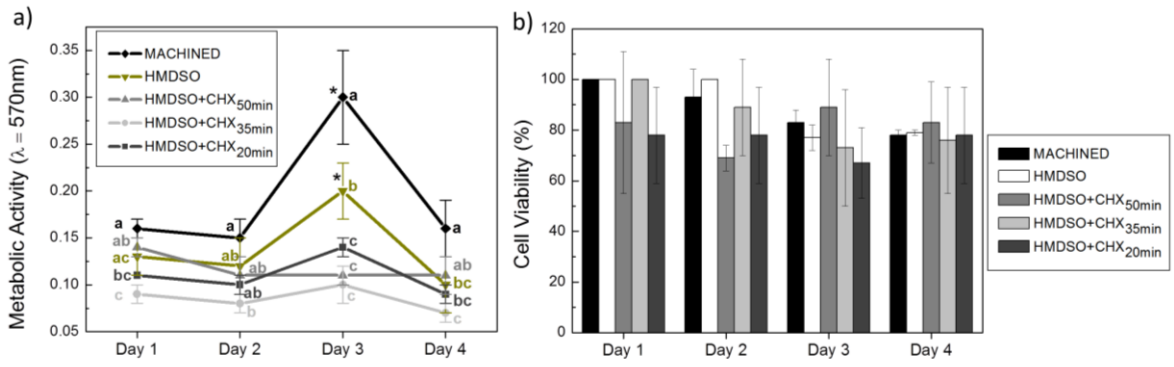

Fig. 9. (a) MTT assay: Cells were seeded at 3×10^4 cells/well and analyzed at 1, 2, 3 and 4 days for the controls and experimental groups (n=9). Asterisk and lower-case letters indicate statistical intra- and inter-group differences ($p<0.05$). **(b)** Cell viability assay: The impact of CHX-doped films created on cpTi discs on cell viability was assessed at 1, 2, 3 and 4 days using the trypan blue dye exclusion assay (n=9). Data is presented as the percentage of viable cells. The error bars indicate standard deviation.

3.7. Cell morphology

In the current study, a potential effect of CHX-doped films based on silicon created on cpTi discs on NIH-F3T3 cell morphology was assessed by SEM (Fig. 10). Overall, qualitative analysis showed that CHX-doped thin films based on silicon did not affect cell adherence onto cpTi discs. However, at the HMDSO+CHX_{20min} group, lower cell densities were observed over the experimental period. Harmful signals of cytotoxic effects and cell death were noted in the HMDSO+CHX_{20min} group as compared to the other groups, including

morphological changes, shrinkage, smaller and pyknotic cells, and loss of cytoplasmic processes. Additionally, at the HMDSO+CHX_{20min} group, cells were found to be arranged in a more sparingly way and small numbers, which might be an indication of cell lysis [52]. This may be attributed to the high concentration of CHX in this group. In contrast, qualitative analysis showed that, at the HMDSO+CHX_{50min} and HMDSO+CHX_{35min} groups, there were not evident differences as compared to the control groups.

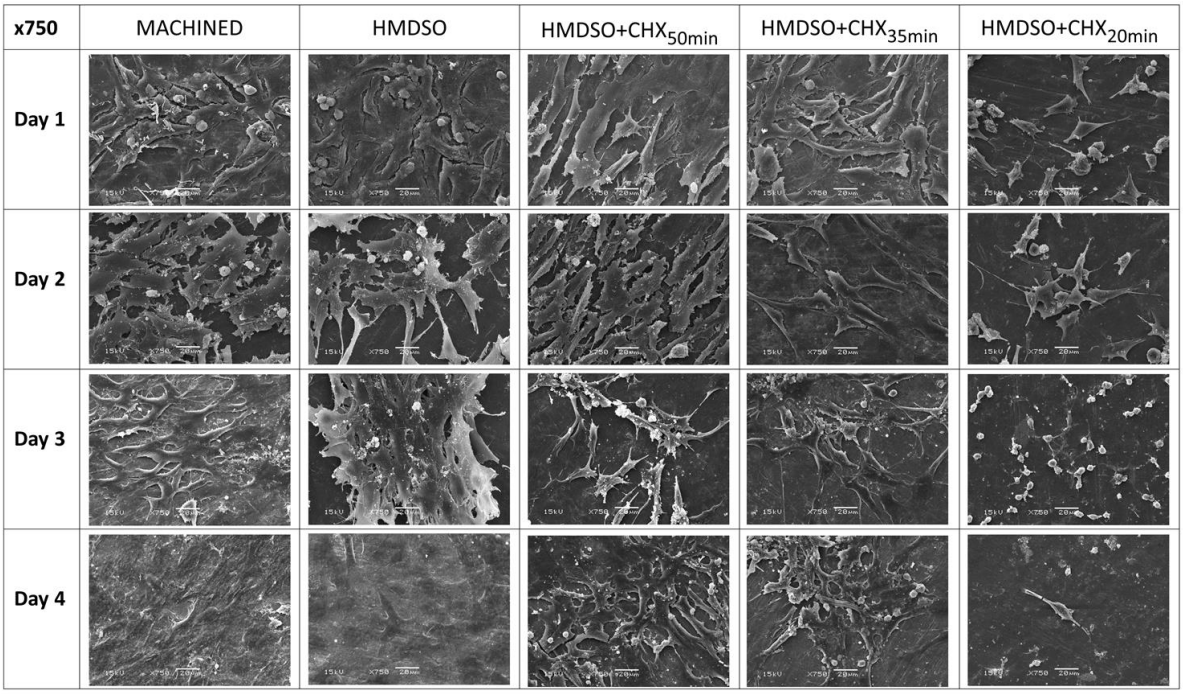

Fig. 10. Scanning electron microscopic micrographs illustrating NIH-F3T3 cells cultured on cpTi discs with and without CHX-doped thin films at days 1, 2, 3 and 4.

3.8. Secretome analysis

Here, the impact of CHX-doped films on the secretion of inflammatory markers was assessed by the multiplex technology. NIH-F3T3 cells were cultured on cpTi discs, with or without CHX-doped thin films, at different period of deposition, and the levels of secreted IL-4, IL-6, IL-17, TNF-α and IFN-y were determined in the culture media. Overall, data analysis demonstrated that films, with or without CHX, significantly affected the expression profile of inflammatory cytokines, including IL-4, IL-6, IL-17, IFN-y and TNF-α by NIH-F3T3 cells as compared to the negative control group ($p<0.05$) (Fig. 11).

Cytokines are proteins released by cells with growth, differentiation and activation functions and are involved in the regulation of inflammatory reactions via a complex mechanism [53]. Fibroblasts act directly on the inflammatory response through tissue

remodeling, acting on bone formation and resorption around the implants [54]. In addition, the activity of commercial proteases and cell-bound bacterial proteases are substantially reduced by CHX [55]. The release of early and late inflammatory mediators and cytokines such as TNF-α, IL-4, IL-6, IL-17, and IFN-y can be reduced by reducing the inflammatory process [56]. Röhner et al. [57] have previously reported that CHX may lead to cell morphological changes and result in the accumulation and secretion of proinflammatory chemokines and cytokines over a short period of time. In the current study, except for IL-6, films with and without CHX led to a fold change increase of all assessed inflammatory markers as compared to the negative control group at all the experimental time points. Intriguingly, an opposite pattern was found for IL-6 that displayed a significant fold change decrease as compared to the bulk cpTi group at all the experimental periods ($p<0.05$).

It is well known that gingival fibroblasts secrete IL-6 during the development of periodontal diseases [58]. IL-6 has been one of the major mediator of host response to injury, inflammation, and infection [59]. However, higher levels of IL-4 affects activated macrophages reducing the effects of TNF-α, and IL-6 inhibiting the production of oxygen free radicals, and is considered a protective factor [60, 61]. IFN-γ has been reported to play a key role on cellular self-activation and [62] as well as an effective macrophage activator [63].

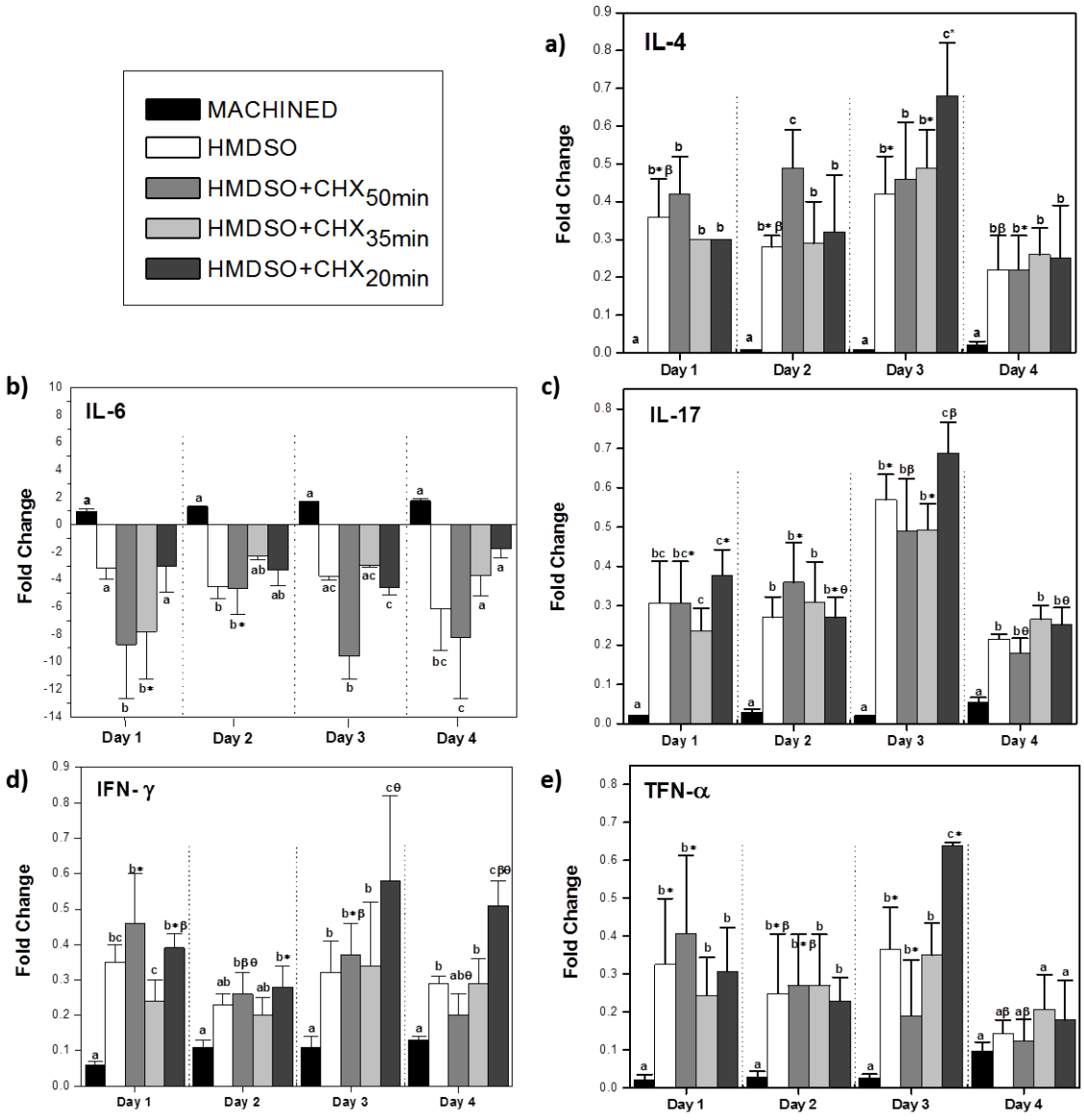

Fig. 11. Release of interleukin IL- 4, IL-6, IL- 17, IFN-Y and TFNα of NIH-F3T3 cells for controls and experimental groups at days 1, 2, 3 and 4 (n=4). Lower case letters indicate significant differences between groups for the same period. *, β and ɵ indicate significant differences in comparison of the different days for the same group ($p<0.05$). The error bars indicate standard deviation.

The healing process around dental implants is directly related to the interaction between biomaterial surfaces and biomarkers [64, 65]. The combination of altered surface chemistry and high surface energy induced macrophages to release greater anti-inflammatory markers and lower of pro-inflammatory markers [66]. In this study, HMDSO+CHX_{50min} and HMDSO+CHX_{35min} groups presented higher surface free energy, and these groups showed

decreased levels of IL-6 when compared to the machined control group. Not only implant topography, but surface wettability is an important factor in decreasing IL-6 expression [67, 68]. In this sense, implant surfaces with greater hydrophilicity present greater adhesion of gingival fibroblasts and reduction of proinflammatory mediators [69]. However, the mechanisms of action are beyond the scope of the current study and remain to be determined.

3.9. Co-culture and analyses of fibroblast cells and S. sanguinis data

For the co-culture model, we used the CHX-doped thin film (HMDSO+CHX_{50min}) that exhibited the most optimized balance between biofilm inhibition and citocompatibility, and compared it with the HMDSO and machined controls. In the WST-1 assay, the HMDSO and HMDSO+CHX_{50min} groups demonstrated the highest metabolic activity values of the fibroblasts and the most constant co-culture growth over the examined period of time, comparable to the machined group. In particular, the HMDSO+CHX_{50min} group was significantly higher than the machined and HMDSO groups at day 3 ($p<0.05$). In contrast, the machined group presented higher metabolic activity of fibroblasts when compared with the HMDSO and

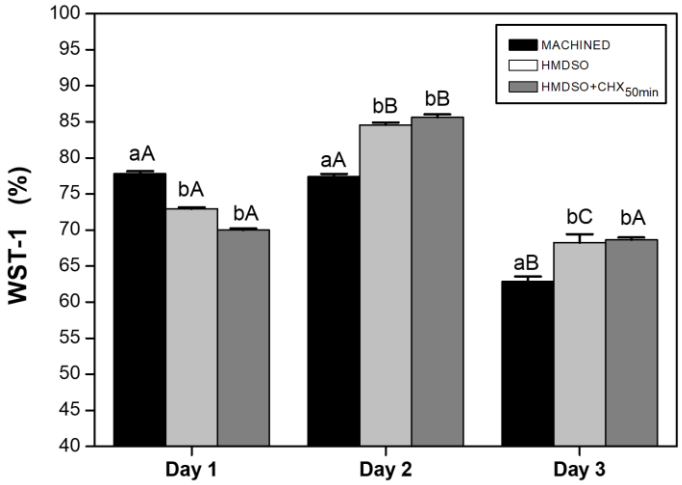

HMDSO+CHX_{50min} groups ($p<0.05$), at early incubation times (Fig. 12).

Fig. 12. WST viability activity of co-culture of periodontal ligament fibroblasts cells and *S. sanguinis* after 24, 48 and 72 h in all groups (n=3). Lower case letters indicate significant differences between groups for the same period. Upper case letters indicate significant differences in comparison of the different days for the same group ($p<0.05$, Tukey HSD test). The error bars indicate standard deviation.

The proliferation and attachment of osteoblast cells has been one of the main factors in the development of new dental implant surfaces, targeted to improve bone formation after implant installation [70]. However, preventing initial infection after implant placement has been considered a major factor in the development of new biomaterial surfaces. Kronstrom et al. [71] reported that early dental implant failure has been commonly associated with primary colonizing bacteria such as *S. sanguinis*, which is commonly involved. These bacteria adhere to any surface, and when colonized on dental implant surfaces may collaborate in the development of peri-implantitis [72].

Therefore, researchers have sought to develop biomaterials with antimicrobial potentials. However, these surfaces could produce toxic effects on the peri-implant region, interfering negatively in the initial implant installation phase [50]. There are standardized methods to identify cell behavior and reactions of tissues to these biomaterials [73]. WST-1 has been used to evaluate biocompatibility of biomaterials due to its reaction with the mitochondrial succinate-tetrazolium reductase forming the formazan dye [74]. Another method commonly used to evaluate biocompatibility of biomaterials is XTT assay, by measuring the mitochondrial activities of cells and microorganisms. XTT is a tetrazolium salt which upon reaction will produce a water soluble formazan derivative [75].

The XTT colorimetric method was used to determine metabolic activity relating to the bacterial cell viability of co-cultured *S. sanguinis* (Fig. 13). In this study, at 1 and 2 days, no differences were observed between all groups; however, the HMDSO+CHX_{50min} group at day 3 exhibited low bacterial metabolic activity of the co-cultured group compared to the machined and HMDSO groups ($p<0.05$).

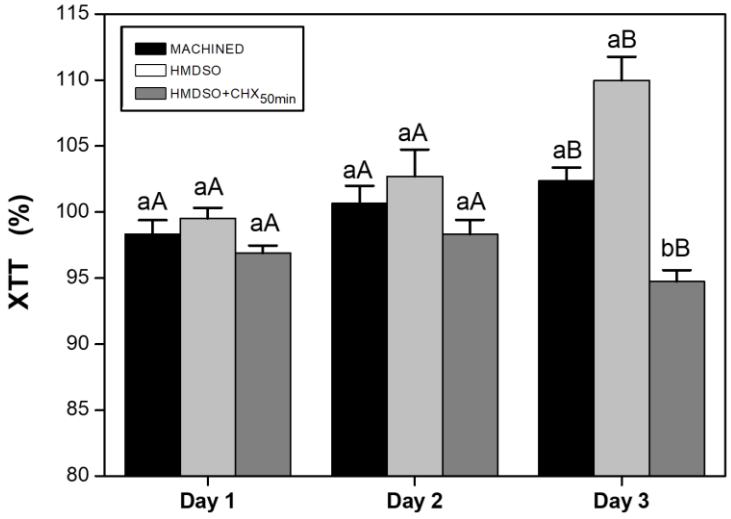

Fig. 13. XTT metabolic activity after exposure of co-culture of periodontal ligament fibroblasts cells and *S. sanguinis* to all groups (n=3). The major reductions in metabolic activity were primarily found to CHX-doped film at day 3 ($p<0.05$), being considered slightly anti-microbial when compared with HMDSO and machined groups. The error bars indicate standard deviation.

Both XTT and WST-1 were used to assess the viability of co-cultured of periodontal ligament fibroblasts cells and *S. sanguinis in vitro* when exposed to the thin film on titanium discs using HMDSO and CHX. The co-cultures grown on the HMDSO+CHX_{50min} group at day 3 demonstrated 94% of maximum metabolic activity with the XTT assay, indicating the co-cultures were viable. Although it was expected that the co-cultures will present low metabolic activity in the HMDSO+CHX_{50min} group, the co-cultures with the HMDSO+CHX_{50min} group exhibited 68% metabolic activity at day 3 for the WST-1 assay without indicating significant differences with the groups without CHX. The WST-1 and XTT assays are complementary, both measuring ability of fibroblast and bacterial cells, respectively, to maintain viability. In this study, the percentage of viability was higher in the XTT assay than the WST-1 assay. The highest viability percentage for the XTT assay can be the combination of the result of a greater number of viable cells, as well as the presence of greater metabolic activity during this analysis [75].

Also, the LDH assay results demonstrated similarity to the other biocompatibility experiments (Fig. 14). The LDH cytotoxicity assay has been widely used to evaluate the presence of toxicity on tissue and human cells. When biomaterials damage cells and cause the

release of LDH, in this colorimetric assay, LDH reduces NAD to NADH, which reacts with the specific probe to generate a fluorescent product [75].

The LDH assay did not indicate an enhancement of LDH activity in the supernatants of co-cultured periodontal ligament fibroblast cells and *S. sanguinis* incubated with the HMDSO+CHX_{50min} group, indicating normal cell vitality. In addition, the measured LDH activity was similar between all groups. However, higher LDH release has previously been described for antimicrobials like CHX [76]. As previously reported, biomaterials with antimicrobial potentials may lead to increased LDH activity present in fibroblast cells, which could have resulted in an increased release of LDH enzyme when the co-culture was exposed to the HMDSO+CHX_{50min} group.

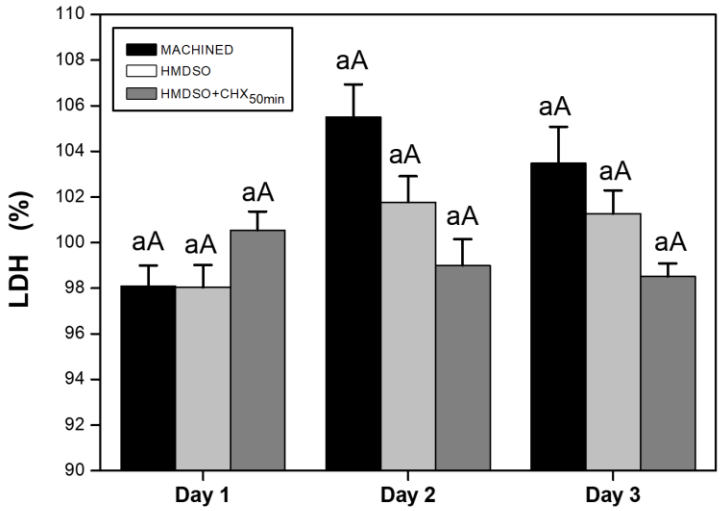

Fig. 14. LDH cytotoxicity activity of co-cultured periodontal ligament fibroblasts cells and *S. sanguinis* after 24, 48 and 72 h in all groups studied (n=3). Lower case letters indicate significant differences between groups for the same period. Upper case letters indicate significant differences in comparison of the different days for the same group. The error bars indicate standard deviation.

Furthermore, the co-cultures were grown for 24, 48 and 72 h, and samples were stained with Live/Dead stain and examined in a confocal microscope. The behavior of bacteria among the three days of incubation may not have provoked a decrease in the number of human periodontal ligament fibroblast cells found on machined and HMDSO groups. On the other hand, HMDSO+CHX_{50min} group exhibited stability in the number of human periodontal ligament fibroblast cells over the three analyzed days, while the number of live

and dead bacteria remained the same (Table 2). In addition, the nuclei of the human periodontal ligament fibroblast cells exposed to the HMDSO+CHX_{50min} group at day 3 exhibited red staining that was not observed in the human periodontal ligament fibroblast cells without CHX (Fig. 15). Although the HMDSO+CHX_{50min} group at day 3 demonstrated a high estimated number of dead *S. sanguinis* cells, in a similar way, the same sample managed to preserve a considerable number of live human periodontal ligament fibroblast cells.

Table 2

Mean number of viable/dead *S. sanguinis* detected (log values) with minimal and maximal data and mean number of human periodontal ligament fibroblast cells after 1, 2 and 3 days of incubation in the co-culture model

	Group	Viable	Dead	Viable		Dead		Fibroblast
		Mean ± SD	Mean ± SD	Min	Max	Min	Max	Mean ± SD
Day 1	Machined	8.1±0.2	7.9±0.1	7.69	8.20	7.74	8.04	15.7±6.5
	HMDSO	7.9±0.2	8.0±0.2	7.76	8.29	7.70	8.32	27.3±3.2
	HMDSO+CHX_{50min}	8.1±0.2	8.2±0.3	7.74	8.45	7.71	8.49	15.7±4.2

	Group	Viable	Dead	Viable		Dead		Fibroblast
		Mean ± SD	Mean ± SD	Min	Max	Min	Max	Mean ± SD
Day 2	Machined	8.0±0.1	8.0±0.2	7.83	8.08	7.84	8.25	31.0±11.7
	HMDSO	7.9±0.2	7.6±0.3	7.65	8.24	7.12	8.04	15.7±5.7
	HMDSO+CHX_{50min}	8.1±0.1	8.0±0.2	8.01	8.31	7.73	8.36	14.3±3.8

	Group	Viable	Dead	Viable		Dead		Fibroblast
		Mean ± SD	Mean ± SD	Min	Max	Min	Max	Mean ± SD
Day 3	Machined	7.4±0.6	6.6±1.5	6.61	7.96	4.63	7.91	51.0±3.0
	HMDSO	7.8±0.3	7.5±0.2	7.50	8.18	7.26	7.73	22.3±7.4
	HMDSO+CHX_{50min}	7.9±0.3	7.8±0.4	7.45	8.23	7.15	8.17	17.3±7.2

It is important that the fitting of peri-implant tissue to the implant contributes to the maintenance of the implant [77]. Although cell damage was observed, this result may not be related to co-infection since *S. sanguinis* are not normally considered pathogenic. Moreover, similar results indicate that osteoblast cells are typically exposed to oral streptococci [78]. In this sense, the lower number of fibroblast cells and the presence of cell damage at day 3 with the HMDSO+CHX_{50min} group is potentially related to the presence of CHX on this surface.

Although CHX has been reported as the gold standard oral antimicrobial agent in the treatment and prevention of a broad spectrum of bacteria. Unfortunately, its use is known to cause undesirable effects, such as low levels of toxicity to oral cavity cells [79].

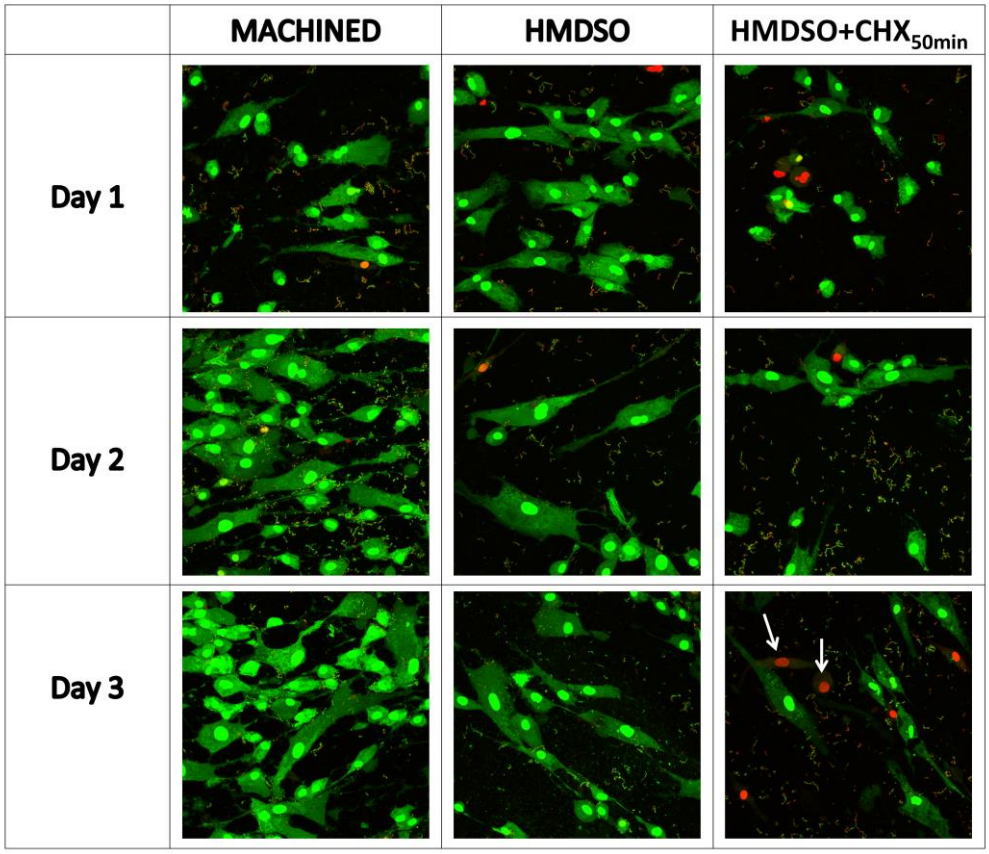

Fig. 15. CLSM images of live/dead staining of co-cultured human periodontal ligament fibroblasts and *S. sanguinis* on all surfaces studied at 1, 2, and 3 days. Live cells are stained in green and dead cells are stained in red. Arrows indicate the red stained nuclei of the human periodontal ligaments fibroblasts cells in red staining.

3.10. Clinical implications, limitations, and future perspectives

Although peri-implant-related disease is host-dependent, bacteria have an important effect in triggering the initial inflammatory process. Topographical and chemical properties of the implant materials have been reported to play a role in biofilm development [80]. The most important discovery in our study is that this new developed multifunctional surface was able to reduce biofilm formation without significantly affecting host cells. Although, we consider GDP as a promising strategy to create bio-functional surfaces, and more specifically modulate biofilm development, the findings of the current study are limited to an *in vitro*

system. Future studies need to evaluate the surface in a location that fully mimics the oral environment in terms of oral fluids such as the protein composition of saliva and blood plasma, and microbiological and cell diversities of the peri-implant site. Additionally, further pre-clinical and controlled clinical *in vivo* studies should be considered in order to confirm CHX-doped thin films based on silicon are a safe, reliable and predictable approach to prevent peri-implantitis.

4. Conclusions

We successfully developed a CHX-doped thin silicon-based film on titanium surface via GDP. CHX thin films remained cytocompatible and reduced *S. sanguinis* biofilm. Therefore, films based of silicon with CHX-created films may potentially represent a significant technological advance to modulate biofilm development on dental- or implant-supported prosthetic structures and to prevent inflammation-associated tissue damage.

Declarations of Competing Interest

None.

Acknowledgments

The authors would like to thank the Sao Paulo Research Foundation (FAPESP) (process numbers 2016/06117-5 and 2017/21894-0) for providing a scholarship to the first author.

References

[1] Rompen E, Domken O, Degidi M, Pontes AE, Piattelli A. The effect of material characteristics, of surface topography and of implant components and connections on soft tissue integration: a literature review. Clinical Oral Implants Research 2006;17 Suppl 2:55-67. doi: 10.1111/j.1600-0501.2006.01367.x

[2] Tomasi C, Tessarolo F, Caola I, Wennstrom J, Nollo G, Berglundh T. Morphogenesis of peri-implant mucosa revisited: an experimental study in humans. Clinical Oral Implants Research 2014;25:997-1003. doi: 10.1111/clr.12223

[3] Lindhe J, Meyle J. Peri-implant diseases: Consensus Report of the Sixth European Workshop on Periodontology. Journal of Clinical Periodontology 2008;35:282-5. doi: 10.1111/j.1600-051X.2008.01283.x

[4] Cortizo MC, Oberti TG, Cortizo MS, Cortizo AM, Fernandez Lorenzo de Mele MA. Chlorhexidine delivery system from titanium/polybenzyl acrylate coating: evaluation of cytotoxicity and early bacterial adhesion. Journal of Dentistry 2012;40:329-37. doi: 10.1016/j.jdent.2012.01.008

[5] Sharma S, Bano S, Ghosh AS, Mandal M, Kim HW, Dey T, et al. Silk fibroin nanoparticles support in vitro sustained antibiotic release and osteogenesis on titanium surface. Nanomedicine 2016;12:1193-204. doi: 10.1016/j.nano.2015.12.385

[6] Lan SF, Kehinde T, Zhang X, Khajotia S, Schmidtke DW, Starly B. Controlled release of metronidazole from composite poly-epsilon-caprolactone/alginate (PCL/alginate) rings for dental implants. Dental Materials 2013;29:656-65. doi: 10.1016/j.dental.2013.03.014

[7] Furst MM, Salvi GE, Lang NP, Persson GR. Bacterial colonization immediately after installation on oral titanium implants. Clinical Oral Implants Research 2007;18:501-8. doi: 10.1111/j.1600-0501.2007.01381.x

[8] Cronan CA, Potempa J, Travis J, Mayo JA. Inhibition of Porphyromonas gingivalis proteinases (gingipains) by chlorhexidine: synergistic effect of Zn(II). Oral Microbiology and Immunology 2006;21:212-7. doi: 10.1111/j.1399-302X.2006.00277.x

[9] Ma S, Niu L, Li F, Fang M, Zhang L, Tay FR, et al. Adhesive Materials with Bioprotective/Biopromoting Functions. Current Oral Health Reports 2014;1:213-21. doi: 10.1007/s40496-014-0027-6

[10] Mensi M, Cochis A, Sordillo A, Uberti F, Rimondini L. Biofilm Removal and Bacterial Re-Colonization Inhibition of a Novel Erythritol/Chlorhexidine Air-Polishing Powder on Titanium Disks. Materials 2018;11. doi: 10.3390/ma11091510

[11] Wang S, Yang Y, Li W, Wu Z, Li J, Xu K, et al. Study of the Relationship Between Chlorhexidine-Grafted Amount and Biological Performances of Micro/Nanoporous Titanium Surfaces. ACS Omega 2019;4:18370-80. doi: 10.1021/acsomega.9b02614
[12] Ryu HS, Kim YI, Lim BS, Lim YJ, Ahn SJ. Chlorhexidine Uptake and Release From Modified Titanium Surfaces and Its Antimicrobial Activity. Journal of Periodontology 2015;86:1268-75. doi: 10.1902/jop.2015.150075
[13] Verraedt E, Braem A, Chaudhari A, Thevissen K, Adams E, Van Mellaert L, et al. Controlled release of chlorhexidine antiseptic from microporous amorphous silica applied in open porosity of an implant surface. International Journal of Pharmaceutics 2011;419:28-32. doi: 10.1016/j.ijpharm.2011.06.053
[14] Bazaka K, Jacob MV, Crawford RJ, Ivanova EP. Plasma-assisted surface modification of organic biopolymers to prevent bacterial attachment. Acta Biomaterialia 2011;7:2015-28. doi: 10.1016/j.actbio.2010.12.024
[15] Chang YC, Feng SW, Huang HM, Teng NC, Lin CT, Lin HK, et al. Surface analysis of titanium biological modification with glow discharge. Clinical Implant Dentistry and Related Research 2015;17:469-75. doi: 10.1111/cid.12141
[16] Wei J, Yoshinari M, Takemoto S, Hattori M, Kawada E, Liu B, et al. Adhesion of mouse fibroblasts on hexamethyldisiloxane surfaces with wide range of wettability. Journal of Biomedical Materials Research Part B, Applied Biomaterials 2007;81:66-75. doi: 10.1002/jbm.b.30638
[17] Ercan UK, Smith J, Ji HF, Brooks AD, Joshi SG. Chemical changes in nonthermal plasma-treated N-acetylcysteine (NAC) solution and their contribution to bacterial inactivation. Scientific Reports 2016;6:20365. doi: 10.1038/srep20365
[18] Pramanik C, Wang T, Ghoshal S, Niu L, Newcomb BA, Liu Y, et al. Microfibrous borate bioactive glass dressing sequesters bone-bound bisphosphonate in the presence of simulated body fluid. Journal of Materials Chemistry B 2015;3:959-63. doi: 10.1039/c4tb02035a
[19] Verraedt E, Pendela M, Adams E, Hoogmartens J, Martens JA. Controlled release of chlorhexidine from amorphous microporous silica. Journal of Controlled Release 2010;142:47-52. doi: 10.1016/j.jconrel.2009.09.022
[20] Barbour ME, Maddocks SE, Wood NJ, Collins AM. Synthesis, characterization, and efficacy of antimicrobial chlorhexidine hexametaphosphate nanoparticles for applications in biomedical materials and consumer products. International Journal of Nanomedicine 2013;8:3507-19. doi: 10.2147/IJN.S50140

[21] Matos AO, Ricomini-Filho AP, Beline T, Ogawa ES, Costa-Oliveira BE, de Almeida AB, et al. Three-species biofilm model onto plasma-treated titanium implant surface. Colloids and Surfaces B, Biointerfaces 2017;152:354-66. doi: 10.1016/j.colsurfb.2017.01.035
[22] Barao VA, Ricomini-Filho AP, Faverani LP, Del Bel Cury AA, Sukotjo C, Monteiro DR, et al. The role of nicotine, cotinine and caffeine on the electrochemical behavior and bacterial colonization to cp-Ti. Materials Science & Engineering C, Materials for Biological Applications 2015;56:114-24. doi: 10.1016/j.msec.2015.06.026
[23] Pereira-Cenci T, Deng DM, Kraneveld EA, Manders EM, Del Bel Cury AA, Ten Cate JM, et al. The effect of Streptococcus mutans and Candida glabrata on Candida albicans biofilms formed on different surfaces. Archives of Oral Biology 2008;53:755-64. doi: 10.1016/j.archoralbio.2008.02.015
[24] Mohd Daud N, Saeful Bahri IF, Nik Malek NAN, Hermawan H, Saidin S. Immobilization of antibacterial chlorhexidine on stainless steel using crosslinking polydopamine film: Towards infection resistant medical devices. Colloids and Surfaces B, Biointerfaces 2016;145:130-9. doi: 10.1016/j.colsurfb.2016.04.046
[25] Jiao K, Niu LN, Li QH, Chen FM, Zhao W, Li JJ, et al. Biphasic silica/apatite co-mineralized collagen scaffolds stimulate osteogenesis and inhibit RANKL-mediated osteoclastogenesis. Acta Biomaterialia 2015;19:23-32. doi: 10.1016/j.actbio.2015.03.012
[26] Lecio G, Ribeiro FV, Pimentel SP, Reis AA, da Silva RVC, Nociti-Jr F, et al. Novel 20% doxycycline-loaded PLGA nanospheres as adjunctive therapy in chronic periodontitis in type-2 diabetics: randomized clinical, immune and microbiological trial. Clinical Oral Investigations 2020;24:1269-79. doi: 10.1007/s00784-019-03005-9
[27] Dabija-Wolter G, Sapkota D, Cimpan MR, Neppelberg E, Bakken V, Costea DE. Limited in-depth invasion of Fusobacterium nucleatum into in vitro reconstructed human gingiva. Archives of Oral Biology 2012;57:344-51. doi: 10.1016/j.archoralbio.2011.09.015
[28] Ohadi M, Forootanfar H, Dehghannoudeh G, Eslaminejad T, Ameri A, Shakibaie M, et al. Antimicrobial, anti-biofilm, and anti-proliferative activities of lipopeptide biosurfactant produced by Acinetobacter junii B6. Microbial Pathogenesis 2020;138:103806. doi: 10.1016/j.micpath.2019.103806
[29] Gomez GF, Huang R, Eckert G, Gregory RL. Effect of phototherapy on the metabolism of Streptococcus mutans biofilm based on a colorimetric tetrazolium assay. Journal of Oral Science 2018;60:242-6. doi: 10.2334/josnusd.17-0203
[30] Beline T, Marques Ida S, Matos AO, Ogawa ES, Ricomini-Filho AP, Rangel EC, et al. Production of a biofunctional titanium surface using plasma electrolytic oxidation and glow-

discharge plasma for biomedical applications. Biointerphases 2016;11:011013. doi: 10.1116/1.4944061
[31] Hayakawa T, Yoshinari M, Nemoto K. Characterization and protein-adsorption behavior of deposited organic thin film onto titanium by plasma polymerization with hexamethyldisiloxane. Biomaterials 2004;25:119-27. doi: 10.1016/s0142-9612(03)00484-8.
[32] Cieplik F, Jakubovics NS, Buchalla W, Maisch T, Hellwig E, Al-Ahmad A. Resistance Toward chlorhexidine in oral bacteria - is there cause for concern? Frontiers in Microbiology 2019;10:587. doi: 10.3389/fmicb.2019.00587
[33] Yasuda H. Plasma polymerization. Orlando: Academic Press; 1985.
[34] Rangel RCC, Cruz NC, Rangel EC. Role of the plasma activation degree on densification of organosilicon films. Materials 2019;13.doi: 10.3390/ma13010025
[35] Quirynen M, Bollen CM. The influence of surface roughness and surface-free energy on supra- and subgingival plaque formation in man. A review of the literature. Journal of Clinical Periodontology 1995;22:1-14. doi: 10.1111/j.1600-051x.1995.tb01765.x.
[36] Almaguer-Flores A, Olivares-Navarrete R, Wieland M, Ximenez-Fyvie LA, Schwartz Z, Boyan BD. Influence of topography and hydrophilicity on initial oral biofilm formation on microstructured titanium surfaces in vitro. Clinical Oral Implants Research 2012;23:301-7. doi: 10.1111/j.1600-0501.2011.02184.x
[37] Kononen M, Hormia M, Kivilahti J, Hautaniemi J, Thesleff I. Effect of surface processing on the attachment, orientation, and proliferation of human gingival fibroblasts on titanium. Journal of Biomedical Materials Research 1992;26:1325-41. doi: 10.1002/jbm.820261006
[38] Reis MCdS, V.R.M.; Sgura, R.; da Cruz, N.C.; Rangel, E.C.; Medeiros, I.S. Surface characteristics and optical properties of plasma deposited films on indirect aesthetic restorative dental materials. Surface & Coatings Technology 2018;348:55-63. doi: 10.1016/j.surfcoat.2018.05.028.
[39] Rupp F, Gittens RA, Scheideler L, Marmur A, Boyan BD, Schwartz Z, et al. A review on the wettability of dental implant surfaces I: theoretical and experimental aspects. Acta Biomaterialia 2014;10:2894-906. doi: 10.1016/j.actbio.2014.02.040
[40] Gill P, Musaramthota V, Munroe N, Datye A, Dua R, Haider W, et al. Surface modification of Ni-Ti alloys for stent application after magnetoelectropolishing. Materials Science & Engineering C, Materials for Biological Applications 2015;50:37-44. doi: 10.1016/j.msec.2015.01.009

[41] Marmur A. Hydro- hygro- oleo- omni-phobic? Terminology of wettability classification. Soft Matter 2012;8:6867-70.doi: 10.1039/c2sm25443c
[42] Yoo EM, Uhm SH, Kwon JS, Choi HS, Choi EH, Kim KM, et al. The study on inhibition of planktonic bacterial growth by non-thermal atmospheric pressure plasma jet treated surfaces for dental application. Journal of Biomedical Nanotechnology 2015;11:334-41. doi: 10.1166/jbn.2015.2030.
[43] Wilson DJ, Rhodes NP, Williams RL. Surface modification of a segmented polyetherurethane using a low-powered gas plasma and its influence on the activation of the coagulation system. Biomaterials 2003;24:5069-81. doi: 10.1016/s0142-9612(03)00423-x.
[44] Mizrak T, Guncu GN, Caglayan F, Balci TA, Aktar GS, Ipek F. Effect of a controlled-release chlorhexidine chip on clinical and microbiological parameters and prostaglandin E2 levels in gingival crevicular fluid. Journal of Periodontology 2006;77:437-43. doi: 10.1902/jop.2006.050105
[45] Daneshmand N, Jorgensen MG, Nowzari H, Morrison JL, Slots J. Initial effect of controlled release chlorhexidine on subgingival microorganisms. Journal of Periodontal Research 2002;37:375-9. doi: 10.1034/j.1600-0765.2002.01003.x
[46] Anitha V, Rajesh P, Shanmugam M, Priya BM, Prabhu S, Shivakumar V. Comparative evaluation of natural curcumin and synthetic chlorhexidine in the management of chronic periodontitis as a local drug delivery: a clinical and microbiological study. Indian Journal of Dental Research 2015;26:53-6. doi: 10.4103/0970-9290.156806
[47] Kim HW, McCloskey BD, Choi TH, Lee C, Kim MJ, Freeman BD, et al. Oxygen concentration control of dopamine-induced high uniformity surface coating chemistry. ACS Applied Materials & Interfaces 2013;5:233-8. doi: 10.1021/am302439g
[48] Hugo WB, Longworth AR. The effect of chlorhexidine on the electrophoretic mobility, cytoplasmic constituents, dehydrogenase activity and cell walls of Escherichia coli and Staphylococcus aureus. Journal of Pharmacy and Pharmacology 1966;18:569-78. doi: 10.1111/j.2042-7158.1966.tb07935.x
[49] Souza JGS, Bertolini M, Costa RC, Cordeiro JM, Nagay BE, de Almeida AB, et al. Targeting pathogenic biofilms: newly developed superhydrophobic coating favors a host-compatible microbial profile on the titanium surface. ACS Applied Materials & Interfaces 2020;12:10118-29. doi: 10.1021/acsami.9b22741
[50] Giannelli M, Chellini F, Margheri M, Tonelli P, Tani A. Effect of chlorhexidine digluconate on different cell types: a molecular and ultrastructural investigation. Toxicology in vitro 2008;22:308-17. doi: 10.1016/j.tiv.2007.09.012

[51] Zhou DW, Garcia AJ. Measurement systems for cell adhesive forces. Journal of Biomechanical Engineering 2015;137:020908. doi: 10.1115/1.4029210
[52] Faria G, Cardoso CR, Larson RE, Silva JS, Rossi MA. Chlorhexidine-induced apoptosis or necrosis in L929 fibroblasts: A role for endoplasmic reticulum stress. Toxicology and Applied Pharmacology 2009;234:256-65. doi: 10.1016/j.taap.2008.10.012
[53] Turner MD, Nedjai B, Hurst T, Pennington DJ. Cytokines and chemokines: At the crossroads of cell signalling and inflammatory disease. Biochimica et biophysica acta 2014;1843:2563-82. doi: 10.1016/j.bbamcr.2014.05.014
[54] Frojd V, Wennerberg A, Franke Stenport V. Importance of Ca(2+) modifications for osseointegration of smooth and moderately rough anodized titanium implants - a removal torque and histological evaluation in rabbit. Clinical Implant Dentistry and Related Research 2012;14:737-45. doi: 10.1111/j.1708-8208.2010.00315.x
[55] Grenier D. Reduction of proteolytic degradation by chlorhexidine. Journal of Dental Research 1993;72:630-3.doi: 10.1177/00220345930720031301
[56] Garlet GP. Destructive and protective roles of cytokines in periodontitis: a re-appraisal from host defense and tissue destruction viewpoints. Journal of Dental Research 2010;89:1349-63. doi: 10.1177/0022034510376402
[57] Rohner E, Hoff P, Gaber T, Lang A, Voros P, Buttgereit F, et al. Cytokine expression in human osteoblasts after antiseptic treatment: a comparative study between polyhexanide and chlorhexidine. Journal of Investigative Surgery 2015;28:1-7. doi: 10.3109/08941939.2014.941445
[58] Takahashi K, Takashiba S, Nagai A, Takigawa M, Myoukai F, Kurihara H, et al. Assessment of interleukin-6 in the pathogenesis of periodontal disease. Journal of Periodontology 1994;65:147-53. doi: 10.1902/jop.1994.65.2.147
[59] Deo V, Bhongade ML. Pathogenesis of periodontitis: role of cytokines in host response. Dentistry Today 2010;29:60-2, 64-6; quiz 68-9.
[60] Martinho FC, Nascimento GG, Leite FR, Gomes AP, Freitas LF, Camoes IC. Clinical influence of different intracanal medications on Th1-type and Th2-type cytokine responses in apical periodontitis. Journal of Endodontics 2015;41:169-75. doi: 10.1016/j.joen.2014.09.028
[61] de Oliveira CM, Sakata RK, Issy AM, Gerola LR, Salomao R. Cytokines and pain. Revista Brasileira de Anestesiologia 2011;61:255-9, 60-5, 137-42. doi: 10.1016/S0034-7094(11)70029-0

[62] Silva TA, Garlet GP, Fukada SY, Silva JS, Cunha FQ. Chemokines in oral inflammatory diseases: apical periodontitis and periodontal disease. Journal of Dental Research 2007;86:306-19. doi: 10.1177/154405910708600403
[63] Collart MA, Belin D, Vassalli JD, de Kossodo S, Vassalli P. Gamma interferon enhances macrophage transcription of the tumor necrosis factor/cachectin, interleukin 1, and urokinase genes, which are controlled by short-lived repressors. Journal of Experimental Medicine 1986;164:2113-8. doi: 10.1084/jem.164.6.2113
[64] Peltroche-Llacsahuanga H, Schmidt S, Schnitzler N, Lutticken R, Haase G. Simultaneous measurement of biopolymer-mediated Mac-1 up-regulation and adherence of neutrophils: a novel flow cytometric approach for predicting initial inflammatory interaction with foreign materials. Journal of Immunological Methods 2001;258:13-25.doi: 10.1016/s0022-1759(01)00468-9
[65] Refai AK, Textor M, Brunette DM, Waterfield JD. Effect of titanium surface topography on macrophage activation and secretion of proinflammatory cytokines and chemokines. Journal of Biomedical Materials Research Part A 2004;70:194-205. doi: 10.1002/jbm.a.30075
[66] Hotchkiss KM, Ayad NB, Hyzy SL, Boyan BD, Olivares-Navarrete R. Dental implant surface chemistry and energy alter macrophage activation in vitro. Clinical Oral Implants Research 2017;28:414-23. doi: 10.1111/clr.12814
[67] Alfarsi MA, Hamlet SM, Ivanovski S. The effect of platelet proteins released in response to titanium implant surfaces on macrophage pro-inflammatory cytokine gene expression. Clinical Implant Dentistry and Related Research 2015;17:1036-47.doi: 10.1111/cid.12231
[68] Hamlet S, Alfarsi M, George R, Ivanovski S. The effect of hydrophilic titanium surface modification on macrophage inflammatory cytokine gene expression. Clinical Oral Implants Research 2012;23:584-90. doi: 10.1111/j.1600-0501.2011.02325.x
[69] Wang X, Wang Y, Bosshardt DD, Miron RJ, Zhang Y. The role of macrophage polarization on fibroblast behavior-an in vitro investigation on titanium surfaces. Clinical Oral Investigations 2018;22:847-57. doi: 10.1007/s00784-017-2161-8
[70] Fan Y, Xiu K, Dong X, Zhang M. The influence of mechanical loading on osseointegration: an animal study. Science in China Series C, Life sciences 2009;52:579-86. doi: 10.1007/s11427-009-0070-z
[71] Kronstrom M, Svenson B, Hellman M, Persson GR. Early implant failures in patients treated with Branemark System titanium dental implants: a retrospective study. International Journal of Oral & Maxillofacial Implants 2001;16:201-7.

[72] Nakazato G, Tsuchiya H, Sato M, Yamauchi M. In vivo plaque formation on implant materials. International Journal of Oral & Maxillofacial Implants 1989;4:321-6.
[73] Weyermann J, Lochmann D, Zimmer A. A practical note on the use of cytotoxicity assays. International Journal of Pharmaceutics 2005;288:369-76. doi: 10.1016/j.ijpharm.2004.09.018
[74] Ngamwongsatit P, Banada PP, Panbangred W, Bhunia AK. WST-1-based cell cytotoxicity assay as a substitute for MTT-based assay for rapid detection of toxigenic Bacillus species using CHO cell line. Journal of Microbiological Methods 2008;73:211-5. doi: 10.1016/j.mimet.2008.03.002
[75] Osorio M, Ortiz I, Ganan P, Naranjo T, Zuluaga R, van Kooten TG, et al. Novel surface modification of three-dimensional bacterial nanocellulose with cell-derived adhesion proteins for soft tissue engineering. Materials Science & Engineering C, Materials for Biological Applications 2019;100:697-705. doi: 10.1016/j.msec.2019.03.045
[76] Ikeda T, Ledwith A, Bamford CH, Hann RA. Interaction of a polymeric biguanide biocide with phospholipid membranes. Biochimica et Biophysica Acta 1984;769:57-66. doi: 10.1016/0005-2736(84)90009-9
[77] Atsuta I, Ayukawa Y, Kondo R, Oshiro W, Matsuura Y, Furuhashi A, et al. Soft tissue sealing around dental implants based on histological interpretation. Journal of Prosthodontic Research 2016;60:3-11. doi: 10.1016/j.jpor.2015.07.001
[78] Dorkhan M, Yucel-Lindberg T, Hall J, Svensater G, Davies JR. Adherence of human oral keratinocytes and gingival fibroblasts to nano-structured titanium surfaces. BMC Oral Health 2014;14:75. doi: 10.1186/1472-6831-14-75
[79] McBain AJ, Bartolo RG, Catrenich CE, Charbonneau D, Ledder RG, Gilbert P. Effects of a chlorhexidine gluconate-containing mouthwash on the vitality and antimicrobial susceptibility of in vitro oral bacterial ecosystems. Applied and Environmental Microbiology 2003;69:4770-6. doi: 10.1128/aem.69.8.4770-4776.2003
[80] Teughels W, Van Assche N, Sliepen I, Quirynen M. Effect of material characteristics and/or surface topography on biofilm development. Clinical Oral Implants Research 2006;17 Suppl 2:68-81.doi: 10.1111/j.1600-0501.2006.01353.x

Credit author statement

Adaias Oliveira Matos: Conceptualization, Methodology, Formal analysis, Investigation, Writing - Original Draft.

Amanda Bandeira de Almeida: Methodology, Investigation, Writing - Review & Editing.

Thamara Beline: Methodology, Investigation, Writing - Review & Editing.

Caroline C Tonon: Methodology, Investigation, Writing - Review & Editing.

Renato Corrêa Viana Casarin: Resources, Writing - Review & Editing.

Lester Jack Windsor: Resources, Writing - Review & Editing.

Simone Duarte: Resources, Writing - Review & Editing.

Francisco Humberto Nociti Junior: Methodology, Resources, Writing - Review & Editing.

Elidiane Cipriano Rangel: Methodology, Resources, Writing - Review & Editing.

Richard Lee Gregory: Methodology, Resources, Writing - Review & Editing.

Valentim Adelino Ricardo Barão: Conceptualization, Writing - Review & Editing, Supervision, Project administration, Funding acquisition.